*Theoretical Notes
Note 273*

*TN 273*

# CABLE RESPONSE SOLUTION TECHNIQUES FOR THE SYSTEM-GENERATED ELECTROMAGNETIC PULSE ENVIRONMENT

Volume 2

Preliminary Estimate of Photon Excitation of Multiconductor Cables

Monte Wilson
Paul Trybus

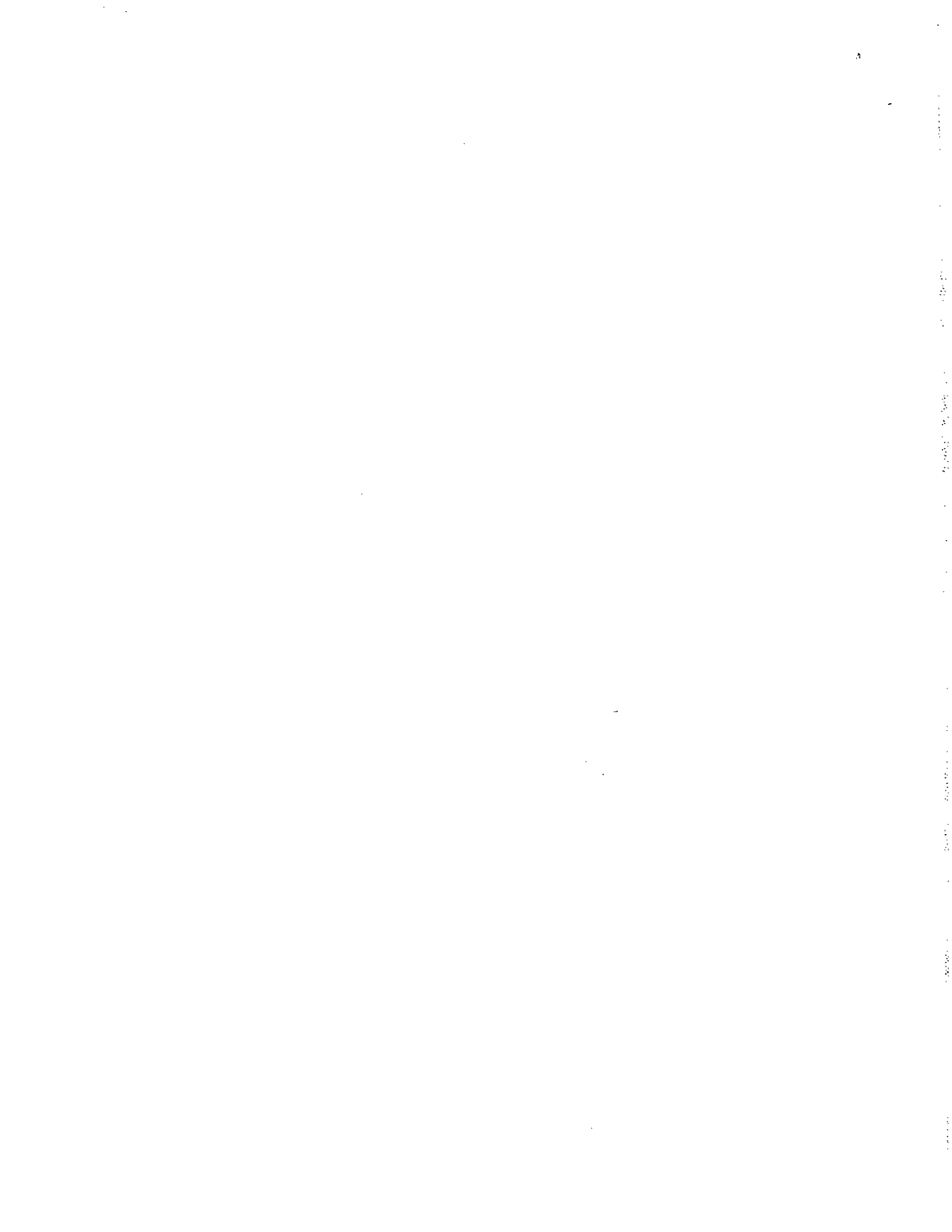Mission Research Corporation
P. O. Box 8693
Albuquerque, NM 87108

May 1976

Final Report

**AIR FORCE WEAPONS LABORATORY**
Air Force Systems Command
Kirtland Air Force Base, NM 87117

| REPORT DOCUMENTATION PAGE | | READ INSTRUCTIONS BEFORE COMPLETING FORM |
|---|---|---|
| 1. REPORT NUMBER <br> AFWL-TR-75-174, Vol. 2 | 2. GOVT ACCESSION NO. | 3. RECIPIENT'S CATALOG NUMBER |
| 4. TITLE *(and Subtitle)* CABLE RESPONSE SOLUTION TECHNIQUES FOR THE SYSTEM-GENERATED ELECTROMAGNETIC PULSE ENVIRONMENT; Vol. 2--Preliminary Estimate of Photon Excitation of Multiconductor Cables | | 5. TYPE OF REPORT & PERIOD COVERED <br> Final Report |
| | | 6. PERFORMING ORG. REPORT NUMBER <br> INTEL-RT 8111-078 |
| 7. AUTHOR(s) <br><br> Monte Wilson <br> Paul Trybus | | 8. CONTRACT OR GRANT NUMBER(s) <br><br> F29601-74-C-0039 |
| 9. PERFORMING ORGANIZATION NAME AND ADDRESS <br> Mission Research Corporation <br> P.O. Box 8693 <br> Albuquerque, New Mexico 87108 | | 10. PROGRAM ELEMENT, PROJECT, TASK AREA & WORK UNIT NUMBERS <br><br> 49950310 |
| 11. CONTROLLING OFFICE NAME AND ADDRESS <br> Air Force Weapons Laboratory <br> Kirtland Air Force Base, NM 87117 | | 12. REPORT DATE <br> May 1976 |
| | | 13. NUMBER OF PAGES <br> 48 |
| 14. MONITORING AGENCY NAME & ADDRESS*(if different from Controlling Office)* | | 15. SECURITY CLASS. *(of this report)* <br><br> UNCLASSIFIED |
| | | 15a. DECLASSIFICATION/DOWNGRADING SCHEDULE |

16. DISTRIBUTION STATEMENT *(of this Report)*

Approved for public release; distribution unlimited.

17. DISTRIBUTION STATEMENT *(of the abstract entered in Block 20, if different from Report)*

18. SUPPLEMENTARY NOTES
This report consists of two volumes: Vol. 1, Methodology and Development of A SGEMP Cable Code, is by Intelcom Rad Tech; and Vol. 2, Preliminary Estimate of Photon Excitation of Multiconductor Cables, presents supporting analysis by Mission Research Corporation

19. KEY WORDS *(Continue on reverse side if necessary and identify by block number)*
System Generated EMP (SGEMP)
Computer Programs
Radiation Effects
Cable Currents
Satellite Systems Analysis

20. ABSTRACT *(Continue on reverse side if necessary and identify by block number)*

Under subcontract to Intelcom Rad Tech, Mission Research Corporation was to provide preliminary analysis of the response of cables to photon excitation to ascertain the significant difference between multiconductor cable response and the more tractable sigle wire cable model. This volume provides the result of that analysis.

DD `FORM 1 JAN 73` 1473    EDITION OF 1 NOV 65 IS OBSOLETE

# TABLE OF CONTENTS

# LIST OF FIGURES

## LIST OF FIGURES (continued)

## LIST OF TABLES

# Section 1

## SUMMARY

The principle thrust of MRC's effort was to determine if the photon induced differential voltages between conductors in a multiconductor cable can be a significant drive term when compared to the common mode excitation of the cable.

Section 2 provides the numerical results of the analysis. Figure S1 shows one of the interesting results of this study. For low impedance loads the differential voltage is always small compared to the common mode voltage (V = -0.02 volt diff/5 volts common mode).
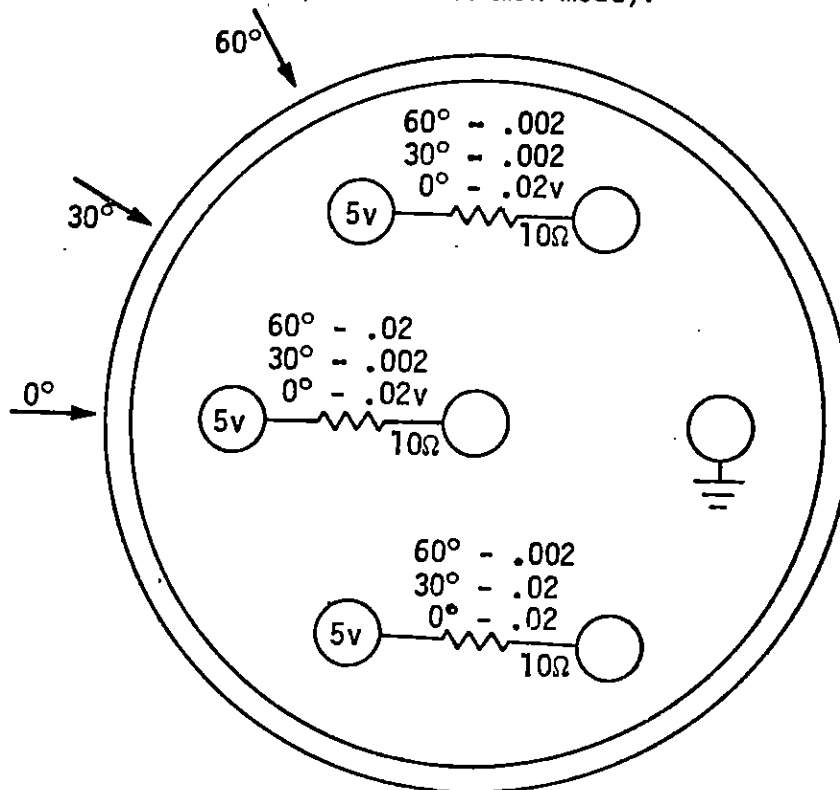


Figure S1. Shadowing Effect on Differential Voltages with Low-Z Loads Normalized to 1 cal/cm² 2 keV BBT X-rays (from Table 5a).

1

For these low energy photons it is the attenuation of the photons in passing through copper wires that is primarily responsible for the differential voltages.

The fact that the differential voltage is this small is due to the low impedance loads assumed here, 10 ohms, and the high impedance source of differential current. These calculations were repeated for an assumed 10 kΩ differential load, then the differential voltages are the same magnitude as the common mode voltage of the illuminated conductor (Table 7) again reflecting the fact that only the directly illuminated conductors are excited.

The conclusion can be drawn that for shielded cables the photon excitation of individual conductors is the dominant drive term for both differential and common mode voltages. This conclusion does not sound very profound to the average reader, however, it is a reversal of the result obtained for electromagnetic coupling, where bulk currents and average common mode voltages are related to the incident E and H field while differential voltages are determined by electromagnetic coupling within the cable and circuit imbalances in the terminations.

MRC's results confirm those of other writers in that vacuum gaps surrounding the insulated wire within a shielded conduction result in large increases in photon induced voltages (Table 9). An interesting note here is that some self-consistent effects could occur within these vacuum gaps at high fluence. However, this does not appear to be a dominant effect because the conductor voltages would only effect the very low energy electrons.

MRC also analyzed the differential voltage expected within un-shielded multiconductor cables supported above an electron emitting ground plane. For this type of cable the principle excitation function is the electron emitted from the ground plane and sticking in the dielec-tric insulation on the wires within the cable. The electrons emitted

2

by the individual wires within the conductor have a smaller effect here than they do in the shielded cable because the capacity to ground is so much smaller. For this case photon excitation is more like the E and H excitation phenomena: the number of electrons striking each wire is not very important in determining its response, and a more important parameter is the termination of the cable and the electromagnetic coupling within the cable.

We also noted that although termination voltages can be large enough to endanger solid state components at reasonably high fluence levels, the peak conductor voltage to ground would still only influence low energy electrons. Consequently, it appears that accurate estimate of cable response can be made without including the self-consistent effects of cable voltage on electron trajectory.

Two other short topics were considered during this study, and that work is also discussed here.

## Section 2

## PRELIMINARY ESTIMATES OF BULK CABLE RESPONSE TO X RAYS

### Monti Wilson

The purpose of the calculation to be described is to obtain preliminary estimates of common mode and differential voltages excited in a bundle of insulated wires (within a coaxial shield or near a ground plane) exposed to x-rays. We consider x-rays from a 2,5,10 and 15 kev blackbody filtered through aluminum or copper (the sheath or wall) and incident on a seven-wire bundle.

Using Dellin-MacCallum [1,2] electron emission sources and simple exponential photon attenuation approximations, current (or voltage) drivers are constructed for input to a time-domain multiconductor transmission line model. Peak terminal line and load voltage predictions are presented parametrically for the case of a short (1 meter) cable segment and an incident $\sin^2$ photon pulse with a FWHM of 10 ns.

### 2.0 TRANSMISSION LINE MODEL FOR A BUNDLE OF INSULATED WIRES WITHIN A COAXIAL SHIELD

The cable model is shown in Figure 1. The metal shield of radius $R_s$ may allow a (vacuum) gap between $R_s$ and $R_b$, the effective outer radius of the bundle.

X rays incident on the cable create two principal driving sources: 1) electrons emitted from the inner shield wall strike and stick in the wire insulation, capacitively coupling current into the wires, 2) electrons emitted from the wires are stopped in the insulating sheaths (of thickness greater than any electron range of interest) and also capacitively couple a time varying wire charge to the ground.

4

Electrons emitted from the insulation and traveling between wires are neglected here to a good first approximation since insulation electron emission is down considerable from the metal photoemission levels. Photo conductivity of the insulation is also neglected.
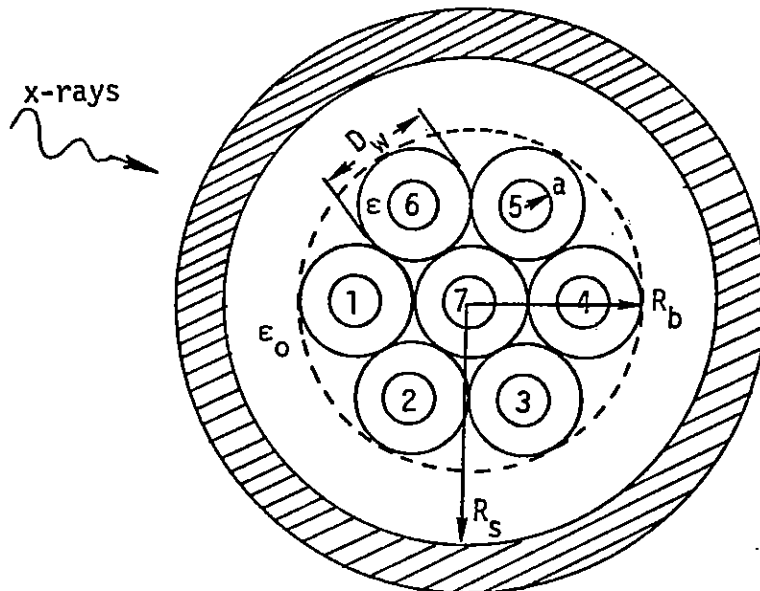


Figure 1.  A bundle of seven identical insulated wires of
radius a within a metal shield.

A transmission line circuit section (representative of each wire i
of the bundle) incorporating these two drivers is shown in Figure 2a.
Figure 2b is a Thevenin equivalent circuit.



(a)

(b)
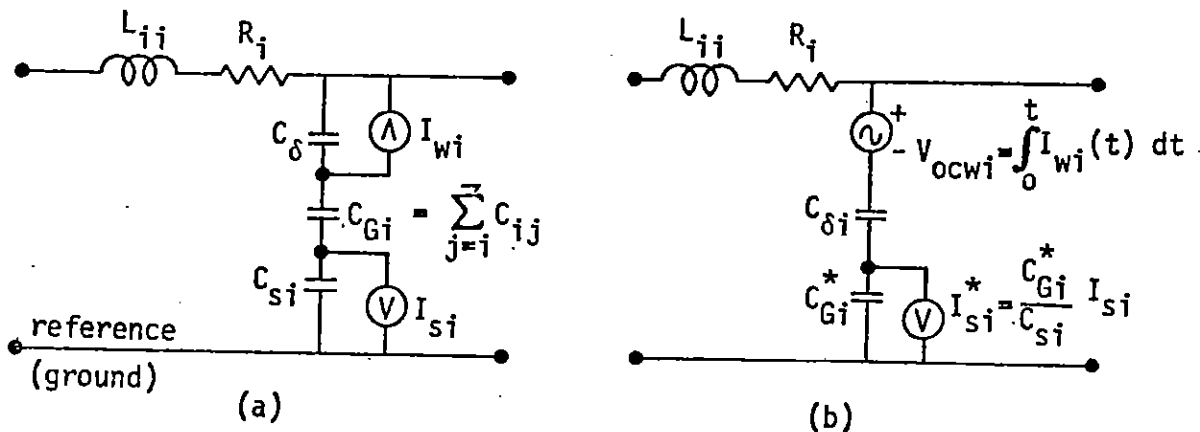
Figure 2.  Transmission Line Circuit Section (a) and Thevenin
Equivalent (b) (Mutual capacitance and inductance not
shown.)

In Figure 2, $I_{wi}$ represents the (conventional) current due to all electrons ejected from wire i into the insulator. These electrons penetrate the insulation to a mean distance <Re> (implying a spectral average). The capacitance of this electron layer is

$$C_{\delta i} = \frac{2\pi\varepsilon}{\ln\left(\frac{a+\langle R_e\rangle_i}{a}\right)}$$

(1)

$C_\delta$ in (1) may be different for each wire since $\langle R_e\rangle$ is dependent on photon attenuation.

In order to treat the electrons from the wall, the shield of Figure 1 is subdivided into 6 sections corresponding to wires 1..6. If $C_{Gi}$ is the total capacitance to ground of the $i^{th}$ wire computed with respect to a reference conductor at radius $R_b$, then the "new" capacitance to ground (Figure 2b) is

$$\frac{1}{C_{Gi}^*} = \frac{1}{C_{Si}} + \frac{1}{C_{Gi}}$$

(2)

where the sheath capacitance in general is

$$C_{Si}_{i<7} = \frac{1}{6} \frac{2\pi}{\frac{\ln(R_s/R_b)}{\varepsilon_0} + \frac{\ln\left((R_b - \langle R_e\rangle_i)/R_b\right)}{\varepsilon}}$$

(3)

In 3, $\langle R_e\rangle_i$ again denotes a mean penetration range of electrons into the insulation.

The current generator $I_{Si}$ shunting $C_{Si}$ is approximated by

$$I_{Si} = J_{wi} \times D_w ,$$

(4)

where $J_{wi}$ is the emission current density of electrons from the wall segment near wire i and $D_w$ is the projected area/unit length for electron capture. The calculation of $I_{wi}$, $\langle R_e\rangle_i$ and $J_{wi}$ is considered in the next section.

For the center wire 7 in Figure 1, the shield quantities are defined as

$$C_{s7} = 6 \times C_{si} \quad (any \ i<7),$$

$$I_{s7} = \sum_{i=1}^{6} I_{si} \qquad (5)$$

From (5) and the equivalent generator $I_{si}^{*}$ in Figure 2b, the center wire is subject to an excitation potential which the mean value for the outer six wires (common mode excitation).

The telegraphers equations to be solved for the Figure 1 cable, using the above sources are

$$\frac{\partial V}{\partial x} = -L \frac{\partial i}{\partial t} - Ri + V_s$$

$$\frac{\partial i}{\partial x} = -C\frac{\partial V}{\partial t} + I_s \ , \qquad (6)$$

where matrix notation is understood and

$$[L] \ [C] = \frac{1}{V_p^2} \ . \qquad (7)$$

The voltage source in Figure 2b is treated by a transformation of variables. The capacitance $C_{\delta i}$ in Figure 2b enters the voltage source $V_{ocwi}$ but is large enough to be neglected in series combination with the other circuit capacitances. The numerical solution of (6) (and the boundary conditions for loaded pairs) is described elsewhere [3].

The capacitance matrix [C] may be calculated by the integral equation method of Licking [4], from which Ezell [5] has abstracted some convenient approximations. In the work, [c] for the model of Figure 1 is calculated for the seven wires within a reference conductor of radius $R_b$, assuming a uniform dielectric medium of permitivity $\varepsilon$. In accord with (2), the original diagonal elements of [C] are then redefined as

$$C_{ii} = C_{Gi}^{*} - \sum_{\substack{J \neq i}}^{7} C_{ij} \ . \qquad (8)$$

## 2.1    ELECTRON EMISSION:  CALCULATION OF $I_{Wi}$, $I_{Si}$, and $<Re>$.

The electron emission sources used here are the bulk photo-Compton currents of Dellin and MacCallum (DM) as computed from the new code QUICKE 2 [2].  The DM bulk currents include photoelectric, Auger and Compton processes and result in electron yields in good ($\leqslant$factor of 2) agreement with both experiment and Monte Carlo predictions.  To estimate the current drivers for the cable of Figure 1, we use the DM sources directly, allowing no field action on emitted electrons.

Tables 1 and 2 show various final source quantities used in the calculations.  The filter (50 mil A$\ell$ or 4 mil Cu) is the shield in the model of Figure 1.

In all cases the emission quantities are averaged over photon angle of incidence, since the variation is small at X-ray energies and unessential to the purpose of these calculations.  The photon angle of incidence enters the cable response calculations through the attenuation of the photon flux by the wires in the bundle.

We treat photon attenuation crudely by interposing integral numbers of wires between source and emission point.  Neglecting the insulation attenuation, each wire contributes a projected mass average attenuation factor

$$g_W(u) = e^{-(\pi/2)\,\rho a \mu_W(u)} \quad , \tag{9}$$

where u is the photon energy, $\mu_W$ the absorption coefficient, $\rho$ the metal density, and a the wire radius.  The shield contributes in all cases a factor

$$g_S(u) = e^{-\mu_S(u) t_S \rho} \quad , \tag{10}$$

where $t_S$ is the nominal thickness of the shield.  Thus $J_{WB3}$ in Table 1 incorporates a total attenuation factor $g_W^3 g_S$.

The $J_{WF}$, $J_{WBi}$ quantities enter the $I_{Si}$ calculation (4).  The individual wire sources are $Q = 2\pi a\, J_{wire}$ charge/unit length, where $J_{wire}$

8

| BB Temp. kev | coulomb/cm²/cal/cm² | | | | $2\pi r\ J_{wire}$ coulomb/cm/cal/cm² | | | $\langle R_{ce}\rangle$ cm | | |
| | $\langle J_{WF}\rangle$ | $\langle J_{WB1}\rangle$ | $\langle J_{WB2}\rangle$ | $\langle J_{WB3}\rangle$ | Intervening Attenuating Wires | | | Intervening Attenuating Wires | | |
| | | | | | 0 | 1 | 2 | 0 | 1 | 2 |
|---|---|---|---|---|---|---|---|---|---|---|
| Cu wires | | | | | | | | | | |
| 2 | $3.32^{-9}$ | $1.09^{-18}$ | $2.24^{-21}$ | $3.50^{-23}$ | $2.10^{-8}$ | $1.68^{-17}$ | $3.75^{-20}$ | $1.76^{-4}$ | $1.86^{-3}$ | $2.61^{-3}$ |
| 5 | $2.78^{-8}$ | $6.17^{-13}$ | $3.18^{-14}$ | $4.54^{-15}$ | $2.02^{-7}$ | $1.09^{-11}$ | $6.32^{-13}$ | $4.12^{-4}$ | $3.25^{-3}$ | $4.54^{-3}$ |
| 10 | $2.78^{-8}$ | $6.09^{-11}$ | $1.14^{-11}$ | $3.31^{-12}$ | $2.31^{-7}$ | $1.25^{-9}$ | $2.51^{-10}$ | $9.46^{-4}$ | $5.04^{-3}$ | $6.12^{-3}$ |
| 15 | $2.00^{-8}$ | $2.34^{-10}$ | $6.81^{-11}$ | $2.83^{-11}$ | $1.77^{-7}$ | $4.97^{-9}$ | $1.46^{-9}$ | $1.60^{-3}$ | $6.21^{-3}$ | $7.63^{-3}$ |
| Al wires | | | | | | | | | | |
| 2 | | $4.79^{-11}$ | $5.30^{-12}$ | $1.61^{-12}$ | $2.65^{-9}$ | $5.34^{-11}$ | $7.06^{-12}$ | $3.15^{-4}$ | $5.40^{-4}$ | $8.07^{-4}$ |
| 5 | | $3.27^{-9}$ | $1.40^{-9}$ | $7.30^{-10}$ | $2.47^{-8}$ | $4.93^{-9}$ | $2.29^{-9}$ | $6.40^{-4}$ | $1.09^{-3}$ | $1.27^{-3}$ |
| 10 | | $7.42^{-9}$ | $4.51^{-9}$ | $3.09^{-9}$ | $2.91^{-8}$ | $1.33^{-8}$ | $8.66^{-9}$ | $1.22^{-3}$ | $1.70^{-3}$ | $1.93^{-3}$ |
| 15 | | $6.84^{-9}$ | $4.78^{-9}$ | $3.66^{-9}$ | $2.26^{-8}$ | $1.33^{-8}$ | $9.84^{-9}$ | $1.70^{-3}$ | $2.18^{-3}$ | $2.42^{-3}$ |

Table 1. Emission quantities and mean electron capacitance spacing $\left(\langle R_{ce}\rangle\right)$ versus blackbody temperature for photons attenuated through 1) 50 mils Al (always) and 2) various numbers of Cu or Al wires. $J_{WF}$ is forward wall emitted charge, $J_{WBi}$ are back wall emitted charges given 1 intervening wires. $r_{wire} = 0.2533$ cm. An average-over photon angle of incidence has been performed.

| BB Temp. kev | coulomb/cm$^2$/cal/cm$^2$ | | | | $2\pi r\, J_{wire}$ coulomb/cm/cal/cm$^2$ | | | $\langle R_{ce}\rangle$ cm | | |
| | $\langle J_{WF}\rangle$ | $\langle J_{WB1}\rangle$ | $\langle J_{WB2}\rangle$ | $\langle J_{WB3}\rangle$ | Intervening Attenuating Wires | | | Intervening Attenuating Wires | | |
| | | | | | 0 | 1 | 2 | 0 | 1 | 2 |
|---|---|---|---|---|---|---|---|---|---|---|
| 2 | $8.67^{-10}$ | $9.52^{-19}$ | $2.06^{-21}$ | $3.29^{-23}$ | $3.53^{-9}$ | $1.47^{-17}$ | $3.46^{-20}$ | $2.00^{-4}$ | $1.87^{-3}$ | $2.62^{-3}$ |
| 5 | $9.23^{-9}$ | $5.77^{-13}$ | $3.06^{-14}$ | $4.43^{-15}$ | $7.28^{-8}$ | $1.02^{-11}$ | $6.09^{-13}$ | $5.99^{-4}$ | $3.28^{-3}$ | $4.55^{-3}$ |
| 10 | $1.51^{-8}$ | $5.88^{-11}$ | $1.12^{-11}$ | $3.26^{-12}$ | $1.34^{-7}$ | $1.21^{-9}$ | $2.47^{-10}$ | $1.25^{-3}$ | $5.07^{-3}$ | $6.14^{-3}$ |
| 15 | $1.31^{-8}$ | $2.29^{-10}$ | $6.72^{-11}$ | $2.81^{-11}$ | $1.23^{-7}$ | $4.86^{-9}$ | $1.44^{-9}$ | $2.02^{-3}$ | $6.24^{-3}$ | $7.66^{-3}$ |

Table 2. Emission quantities and mean electron capacitance spacing $\langle R_{ce}\rangle$ versus blackbody temperature for photons attenuated through 1) 4 mils Cu (always) and 2) various numbers of Cu wires. $\langle J_{WF}\rangle$ is forward wall emitted charge, $J_{WBi}$ are back wall emitted charges given i intervening wires. $r_{wire} = 0.2533$ cm. An average-over photon angle of incidence has been performed.

is a mean radial emission current.  Q is calculated as $\pi a$ × (back current on source side + forward current on shadow side).

The mean electron range $(R_{ce})$ required for (1) and (3) is obtained here from

$$< C_e> = \frac{2\pi\varepsilon}{\ln\left(\frac{a + <R_{ce}>}{a}\right)} = \frac{<Q>}{\left\langle\frac{Q}{C_e}\right\rangle} \quad , \tag{11}$$

where <> denotes integration over the blackbody spectrum.  The range $R_e(u)$ that enters the denominator of (11) is essentially the Berger-Seltzer [6] path length multiplied by an energy dependent factor accounting for multiple scattering (straggling).  This range and hence the layer capacitance (11) will vary according to the spectrum hardness (Tables 1 and 2).

In comparing the Table 1 and 2 quantities it is helpful to keep in mind the blackbody spectrum.  The normalized number spectrum versus energy is characterized in Table 3.

2.2        NUMERICAL RESULTS
The cable bundle considered has dimensions (Figure 1):

$R_b$ = 1 cm

a   = .2533 cm

insulation (polyethylene) thickness - .08 cm

$\varepsilon = 2.3 \, \varepsilon_o$

other dimensions and parameters are indicated on the tables.  Figure 3 shows the resistive load configuration:

11

| u(keV) | $S_2(u)$ | $S_5(u)$ | $S_{10}(u)$ | $S_{15}(u)$ |
|--------|----------|----------|-------------|-------------|
| 1 | $8.01^{-2}$ | $1.50^{-2}$ | $3.95^{-3}$ | $1.79^{-3}$ |
| 5 | $1.16^{-1}$ | $4.84^{-2}$ | $1.60^{-2}$ | $7.79^{-3}$ |
| 10 | $3.53^{-2}$ | $5.21^{-2}$ | $2.42^{-2}$ | $1.30^{-2}$ |
| 20 | $9.44^{-4}$ | $2.48^{-2}$ | $2.60^{-2}$ | $1.76^{-2}$ |
| 30 | $1.43^{-5}$ | $7.44^{-3}$ | $1.96^{-2}$ | $1.74^{-2}$ |
| 50 | $1.80^{-9}$ | $3.78^{-4}$ | $7.05^{-3}$ | $1.14^{-2}$ |
| 100 | $1.00^{-19}$ | $6.86^{-8}$ | $1.88^{-4}$ | $1.57^{-3}$ |
| 150 | $3.13^{-30}$ | $7.00^{-12}$ | $2.86^{-6}$ | $1.26^{-4}$ |
| 300 | $3.36^{-62}$ | $2.62^{-24}$ | $3.50^{-12}$ | $2.29^{-8}$ |

Table 3. Blackbody spectrum (photon/keV) versus photon energy u for temperatures 2, 5, 10, and 15 keV.

Each terminal 1,2,3,5,6,7 has the following open load to ground.
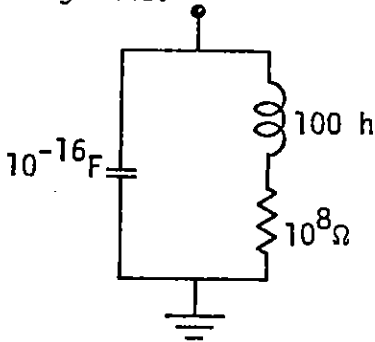
$V_{65}$, $V_{17}$, $V_{23}$ are voltages across the load resistor.
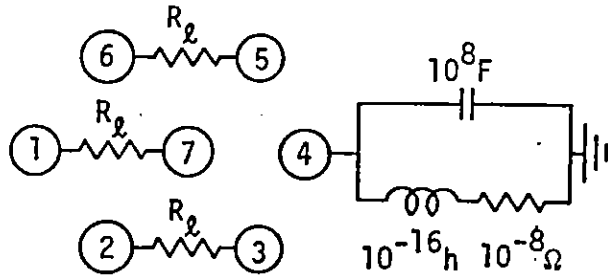
Figure 3.  Resistive load configuration (identical terminations at both ends of cable).

The emission sources in Tables 1 and 2 may be multiplied by a normalized time function. We choose here

$$f(t) = \frac{2}{t_0} \sin^2(\pi t/t_0) \tag{12}$$

$$t_0 = 20 \text{ ns}$$

A cable length of 1 meter was employed, and in all cases the conductor voltages followed the time integral of the source current $I_s$ in (6), reaching peak values well before 30 ns.  The differential load voltages followed the pulse (12).  Only peak voltages are given in the tables to follow.

## 2.2.1  Photon Angle of Incidence

Table 4 illustrates the shadowing assumptions made for 0°, 30°, and 60° photon angle of incidence.  While these assumptions may appear somewhat arbitrary, the scheme serves to vary considerably the photon exposure of each wire in a loaded pair.

13

| Angle of Incidence | Wire | Number of intervening wires for attenuation to the given wire | Number of intervening wires for attenuation to back wall |
|---|---|---|---|
| 0° photons | 1- | 0 | 0 |
| | 2- | 0 | 0 |
| | 3- | 1 | 2 |
| | 4- | 2 | 3 |
| | 5- | 1 | 2 |
| | 6- | 0 | 0 |
| | 7- | 1 | 0 |
| 60° photons | 1- | 0 | 0 |
| | 2- | 1 | 2 |
| | 3- | 2 | 3 |
| | 4- | 1 | 2 |
| | 5- | 0 | 0 |
| | 6- | 0 | 0 |
| | 7- | 1 | 0 |
| 30° photons | 1- | 0 | 0 |
| | 2- | 0 | 0 |
| | 3- | 1 | 2 |
| | 4- | 1 | 2 |
| | 5- | 1 | 0 |
| | 6- | 0 | 0 |
| | 7- | 0 | 0 |

Table 4.   Photon attenuation model for three angles of incidence. The "number of intervening wires" corresponds to the emission quantities $\langle J_{WBi} \rangle$, $\langle 2\pi r\, J_{wire} \rangle$, and the mean electron ranges $\langle R_{ce} \rangle$ in Tables 1 and 2.

14

## 2.2.2 Shielded Bundle Response

The peak terminal voltages with respect to ground and differential load voltages for various fluence levels, shield material, load resistances, photon angle of incidence and distance of shield from the bundle radius are displayed versus the x-ray source blackbody temperature in Figures 5a to 9. In certain cases, the cable sources for electrons ejected from the wires (voltage source $V_{ocwi}$ in Figure 2b) are turned off to see the effect of the shield drivers alone.

Consider first a high fluence level (1 cal/cm$^2$) incident on cables with no gap between $R_s$ and $R_b$ (Figure 1) as in Tables 5a, 6, and 7. With 10Ω loads and a 50 mil aluminum shield (T5a), the differential |voltages| are all ≲1.5 volts, the larger values occurring with the hotter ≥10 kev spectra. The corresponding values given the 4 mil copper shield (T6) are only slightly smaller in magnitude.

The approximate open circuit voltages across 10 kΩ loads (T7) are substantial. Note especially that the shield currents contribute little to the differential voltages. This is due to the large values of $C_{si}$ in (3).

In the no gap cable, essentially all of the important electrons are slowing down in condensed matter (insulation), hence self-consistent effects should be negligible. Of course, the electrons jumping between the air spaces in Figure 1 may be seriously affected by the fields, but the low emission rate for these polyethylene ejected electrons in comparison with the metal sources would seemingly preclude any major perturbations to these simple estimates.

This conclusion should be verified, but an extension of the present model will be required. Since the differential voltages can be of order 10$^2$, particular attention should be paid in such a future investigation to the retardation or enhancement of low ≲100 eV electron emission between insulated wires, though little experimental or theoretical data is available regarding this emission contribution.

Evidently, a "no-gap" shield of "normal" thickness offers little protection to the bundle, at least in the high fluence cases with a

15

| Incidence Angle | Voltage Source $V_{ocwi}$ | BB Temp keV | Peak Differential Voltages $V_{ij} = V_i - V_j$ | | | Peak Conductor Voltages | | |
|---|---|---|---|---|---|---|---|---|
| | | | $V_{17}$ | $V_{23}$ | $V_{65}$ | $V_1$ | $V_2$ | $V_5$ |
| 0° | on | 2 | -.019 | -.015 | -.015 | 4.22 | 5.17 | 5.19 |
| | | 5 | -.435 | -.356 | -.356 | 98.7 | 120 | 120 |
| | | 10 | -1.14 | -.936 | -.937 | 266 | 319 | 320 |
| | | 15 | -1.46 | -1.20 | -1.20 | 360 | 428 | 429 |
| 0° | off | 2 | .0013 | .0016 | .0016 | -1.12 | -.877 | -.878 |
| | | 5 | .026 | .031 | .031 | -21.9 | -17.2 | -17.2 |
| | | 10 | .061 | .071 | .071 | -50.3 | -39.5 | -39.5 |
| | | 15 | .074 | .087 | .087 | -61.5 | -48.3 | -48.4 |
| 30° | on | 2 | -.0010 | -.014 | .0003 | 9.51 | 4.63 | 9.76 |
| | | 5 | -.025 | -.323 | .0048 | 219 | 107 | 225 |
| | | 10 | -.069 | -.852 | -.0096 | 579 | 288 | 597 |
| | | 15 | -.094 | -1.10 | -.0074 | 758 | 386 | 783 |
| 60° | on | 2 | -.017 | -.0014 | -.0014 | 5.48 | .374 | 10.6 |
| | | 5 | -.382 | -.033 | -.033 | 127 | 9.30 | 244 |
| | | 10 | -1.00 | -.088 | -.087 | 340 | 27.5 | 647 |
| | | 15 | -1.29 | -.123 | -.114 | 451 | 45.9 | 846 |

Table 5a. Cable Response. Incident fluence 1 cal/cm$^2$, shield 50 mils aluminum, copper wires, 10Ω loads, $R_s = R_b$ (Figure 1) = 1 cm.

16

| Incidence Angle | Voltage Source $V_{ocwi}$ | BB Temp keV | Peak Differential Voltages $V_{ij} = V_i - V_j$ | | | Peak Conductor Voltages | | |
|---|---|---|---|---|---|---|---|---|
| | | | $V_{17}$ | $V_{23}$ | $V_{65}$ | $V_1$ | $V_2$ | $V_5$ |
| 0° | on | 2 | 1.94 | 2.48 | 2.47 | $-1.69^3$ | $-1.54^3$ | $-1.54^3$ |
| | | 5 | 15.9 | 20.5 | 20.4 | $-1.41^4$ | $-1.28^4$ | $-1.29^4$ |
| | | 10 | 15.2 | 19.8 | 19.7 | $-1.41^4$ | $-1.27^4$ | $-1.27^4$ |
| | | 15 | 10.3 | 13.6 | 13.5 | $-1.01^4$ | $-9.00^3$ | $-9.01^3$ |
| 0° | off | 2 | 1.96 | 2.50 | 2.49 | $-1.69^3$ | $-1.54^3$ | $-1.55^3$ |
| | | 5 | 16.4 | 20.9 | 20.9 | $-1.42^4$ | $-1.30^4$ | $-1.30^4$ |
| | | 10 | 16.4 | 21.0 | 20.9 | $-1.42^4$ | $-1.30^4$ | $-1.30^4$ |
| | | 15 | 11.8 | 15.1 | 15.1 | $-1.03^4$ | $-9.39^3$ | $-9.40^3$ |
| 30° | on | 2 | 1.73 | 2.61 | 1.06 | $-2.10^3$ | $-1.74^3$ | $-2.46^3$ |
| | | 5 | 14.5 | 21.6 | 8.92 | $-1.75^4$ | $-1.45^4$ | $-2.05^4$ |
| | | 10 | 14.5 | 20.9 | 8.95 | $-1.71^4$ | $-1.44^4$ | $-2.01^4$ |
| | | 15 | 10.5 | 14.3 | 6.47 | $-1.20^4$ | $-1.02^4$ | $-1.42^4$ |
| 60° | on | 2 | 1.58 | .88 | .87 | $-1.69^3$ | $-823$ | $-2.26^3$ |
| | | 5 | 12.9 | 7.38 | 7.34 | $-1.41^4$ | $-6.90^3$ | $-1.88^4$ |
| | | 10 | 12.2 | 7.39 | 7.35 | $-1.39^4$ | $-6.90^3$ | $-1.84^4$ |
| | | 15 | 8.15 | 5.31 | 5.30 | $-9.91^3$ | $-4.99^3$ | $-1.29^4$ |

Table 5b. Cable Response. Incident fluence 1 cal/cm$^2$, shield 50 mils aluminum, copper wires, 10$\Omega$ loads, $R_s$ (Figure 1) = 1.2 cm.

| Incidence Angle | Voltage Source $V_{ocwi}$ | BB Temp keV | Peak Differential Voltages $V_{ij} = V_i - V_j$ | | | Peak Conductor Voltages | | |
|---|---|---|---|---|---|---|---|---|
| | | | $V_{17}$ | $V_{23}$ | $V_{65}$ | $V_1$ | $V_2$ | $V_5$ |
| 0° | on | 2 | $-3.5^{-3}$ | $-2.8^{-3}$ | $-2.8^{-3}$ | .69 | .89 | .89 |
| | | 5 | -.23 | -.19 | -.19 | 52.3 | 63.1 | 63.2 |
| | | 10 | -.87 | -.72 | -.72 | 208 | 248 | 249 |
| | | 15 | -1.26 | -1.04 | -1.04 | 320 | 378 | 379 |
| 0° | off | 2 | $4.0^{-4}$ | $4.7^{-4}$ | $4.7^{-4}$ | -.33 | -.26 | -.26 |
| | | 5 | .013 | .015 | .015 | -10.6 | -8.28 | -8.29 |
| | | 10 | .044 | .051 | .051 | -36.0 | -28.3 | -28.3 |
| | | 15 | .061 | .071 | .071 | -50.5 | -39.7 | -39.8 |
| 30° | on | 2 | $-1.3^{-4}$ | $-2.5^{-3}$ | $9.1^{-5}$ | 1.67 | .78 | 1.70 |
| | | 5 | -.013 | -.017 | $2.2^{-3}$ | 115 | 56.8 | 119 |
| | | 10 | $-5.5^{-2}$ | -.66 | $-6.2^{-3}$ | 448 | 224 | 462 |
| | | 15 | -.084 | -.95 | $-4.5^{-3}$ | 661 | 341 | 683 |
| 60° | on | 2 | $-3.1^{-3}$ | $-2.5^{-4}$ | $-2.5^{-4}$ | .93 | .042 | 1.87 |
| | | 5 | -.200 | -.017 | -.017 | 67.2 | 5.07 | 129 |
| | | 10 | -.77 | -.069 | -.067 | 264 | 22.5 | 500 |
| | | 15 | -1.11 | -.11 | -.099 | 397 | 44.6 | 737 |

Table 6.  Cable Response.  Incident fluence 1 cal/cm$^2$, shield 4 mils copper, copper wires, 10Ω loads.  $R_s = R_b$ (Figure 1) = 1 cm.

18

| Voltage Source $V_{ocwi}$ | BB Temp keV | Peak Differential Voltages $V_{ij} = V_i - V_j$ | | | Peak Conductor Voltages | | |
|---|---|---|---|---|---|---|---|
| | | $V_{17}$ | $V_{23}$ | $V_{65}$ | $V_1$ | $V_2$ | $V_5$ |
| on | 2 | 10.4 | 10.8 | 10.8 | 9.72 | 9.91 | - .17 |
| | 5 | 237 | 231 | 231 | 224 | 228 | -2.83 |
| | 10 | 620 | 607 | 607 | 595 | 604 | -1.87 |
| | 15 | 793 | 777 | 777 | 783 | 793 | 17.0 |
| off | 2 | -.69 | -1.04 | -1.04 | -1.52 | -1.39 | - .35 |
| | 5 | -13.6 | -20.4 | -20.4 | -29.9 | -27.2 | -6.79 |
| | 10 | -31.3 | -46.7 | -46.7 | -68.7 | -62.4 | -15.6 |
| | 15 | -38.2 | -56.9 | -56.9 | -84.0 | -76.2 | -19.3 |

Table 7. Cable Response. Incident fluence 1 cal/cm$^2$, shield 50 mils aluminum, copper wires, 10KΩ loads, $R_s = R_b$ (Figure 1) = 1 cm, incidence angle= 0.

blackbody source temperature $\gtrsim 5$ keV. Table 8a shows the very small differential voltages (compared with Table 5a) developed across 10 ohms at a fluence level of 0.1 cal/cm$^2$.

The photon angle of incidence is important in these examples due to the significant attenuation of even a single copper wire of the size we consider. Compare, for example, in Table 5a, the (15 keV BB) voltage $V_{65}$ between cases 0° and 60°. In the 0° case, wire 6 gets a full voltage source while the voltage source for 5 is greatly reduced. This source imbalance leads to a larger $|V_{65}|$ than in the 60° case where equal voltage sources appear on both wires and the differential voltage is developed primarily through the remaining <u>circuit</u> imbalance.

The numbers in Tables 5 to 9 were actually obtained from a preliminary version of the cable model of Figure 2 in which the mean electron ranges $R_{ce}$ were the same for all wire of the bundle. Subsequent investigation indicated, as shown in Tables 1 and 2, that $\langle R_{ce} \rangle$ can differ by as much as an order of magnitude due to wire attenuation. Note, however, that although the wire voltage sources are $\propto \langle R_{ce} \rangle$ for $\langle R_{ce} \rangle \ll r_{wire}$, the current $I_{si}$ for copper wires is reduced significantly by even one wire attenuation factor. The single case of the close shield at high fluence (Table 5a) was recalculated with "wire dependent" $\langle R_{ce} \rangle$, and the results for $V_i$ and $V_{ij}$ were found to agree well (factor of two in a few instances, usually much closer) with the "single $\langle R_{ce} \rangle$" calculations. The remaining cases were not recalculated in order to conserve computer time since the differences should be comparable to the test case. Any future calculations along the lines of Tables 5 to 9 will include the "varying $\langle R_{ce} \rangle$" and additional refinements. The calculations presented here which are "complete" with respect to code development are summarized in Tables 10 and 11. In particular, voltage drops across R in the RLC terminations are included, and somewhat more realistic circuit parameters are employed.

| Incidence Angle | Voltage Source $V_{ocwi}$ | BB Temp keV | Peak Differential Voltages $V_{ij} = V_i - V_j$ | | | Peak Conductor Voltages | | |
|---|---|---|---|---|---|---|---|---|
| | | | $V_{17}$ | $V_{23}$ | $V_{65}$ | $V_1$ | $V_2$ | $V_5$ |
| 0° | on | 2 | $-1.91^{-3}$ | $-1.55^{-3}$ | $-1.55^{-3}$ | .42 | .52 | .52 |
| | | 5 | $-.043$ | $-.035$ | $-.035$ | 9.87 | 11.9 | 12.0 |
| | | 10 | $-.11$ | $-.094$ | $-.094$ | 26.6 | 31.9 | 32.0 |
| | | 15 | $-.15$ | $-.12$ | $-.12$ | 36.0 | 42.8 | 42.9 |
| 0° | off | 2 | $1.36^{-4}$ | $1.58^{-4}$ | $1.58^{-4}$ | $-.11$ | $-.088$ | $-.088$ |
| | | 5 | $2.66^{-3}$ | $3.1^{-3}$ | $3.1^{-3}$ | $-2.19$ | $-1.72$ | $-1.72$ |
| | | 10 | $6.11^{-3}$ | $7.12^{-3}$ | $7.12^{-3}$ | $-5.03$ | $-3.95$ | $-3.95$ |
| | | 15 | $7.45^{-3}$ | $8.71^{-3}$ | $8.70^{-3}$ | $-6.15$ | $-4.83$ | $-4.84$ |
| 30° | on | 2 | $-1.03^{-4}$ | $-1.41^{-3}$ | $2.64^{-5}$ | .95 | .46 | .98 |
| | | 5 | $-2.5^{-3}$ | $-.032$ | $4.83^{-4}$ | 21.9 | 10.7 | 22.5 |
| | | 10 | $-6.95^{-3}$ | $-.085$ | $-9.64^{-4}$ | 57.9 | 28.8 | 59.7 |
| | | 15 | $-9.43^{-3}$ | $-.11$ | $-7.5^{-4}$ | 75.8 | 38.6 | 78.3 |
| 60° | on | 2 | $-1.68^{-3}$ | $-1.42^{-4}$ | $-1.43^{-4}$ | .55 | .037 | 1.06 |
| | | 5 | $-.038$ | $-3.28^{-3}$ | $-3.29^{-3}$ | 12.7 | .93 | 24.4 |
| | | 10 | $-.10$ | $-8.85^{-3}$ | $-8.72^{-3}$ | 34.0 | 2.75 | 64.7 |
| | | 15 | $-.13$ | $-.012$ | $-.011$ | 45.1 | 4.59 | 84.6 |

Table 8a. Cable Response. Incident fluence 0.1 cal/cm$^2$, shield 50 mils aluminum, copper wires, 10 k$\Omega$ loads. $R_s$ (Figure 1) = 1.2 cm.

| Incidence Angle | Voltage Source $V_{ocwi}$ | BB Temp keV | Peak Differential Voltages $V_{ij} = V_i - V_j$ | | | Peak Conductor Voltages | | |
|---|---|---|---|---|---|---|---|---|
| | | | $V_{17}$ | $V_{23}$ | $V_{65}$ | $V_1$ | $V_2$ | $V_5$ |
| 0° | on | 2 | .19 | .25 | .25 | -169 | -154 | -154 |
| | | 5 | 1.59 | 2.05 | 2.04 | $-1.41^{3}$ | $-1.28^{3}$ | $-1.29^{3}$ |
| | | 10 | 1.52 | 1.98 | 1.97 | $-1.41^{3}$ | $-1.27^{3}$ | $-1.27^{3}$ |
| | | 15 | 1.03 | 1.36 | 1.35 | $-1.01^{3}$ | -900 | -901 |
| 0° | off | 2 | .19 | .25 | .25 | -169 | -154 | -155 |
| | | 5 | 1.64 | 2.09 | 2.09 | $-1.42^{3}$ | $-1.30^{3}$ | $-1.30^{3}$ |
| | | 10 | 1.64 | 2.10 | 2.09 | $-1.42^{3}$ | $-1.30^{3}$ | $-1.30^{3}$ |
| | | 15 | 1.18 | 1.51 | 1.51 | $-1.03^{3}$ | -939 | -941 |
| 30° | on | 2 | .17 | .26 | .11 | -210 | -174 | -246 |
| | | 5 | 1.45 | 2.16 | .89 | $-1.75^{3}$ | $-1.45^{3}$ | $-2.05^{3}$ |
| | | 10 | 1.45 | 2.09 | .89 | $-1.71^{3}$ | $-1.43^{3}$ | $-2.01^{3}$ |
| | | 15 | 1.05 | 1.43 | .65 | $-1.20^{3}$ | $-1.02^{3}$ | $-1.42^{3}$ |
| 60° | on | 2 | .16 | .088 | .087 | -169 | -82.3 | -226 |
| | | 5 | 1.29 | .74 | .73 | $-1.41^{3}$ | -690 | $-1.88^{3}$ |
| | | 10 | 1.22 | .74 | .73 | $-1.39^{3}$ | -690 | $-1.84^{3}$ |
| | | 15 | .81 | .53 | .53 | -991 | -499 | $-1.29^{3}$ |

Table 8b. Cable Response. Incident fluence 0.1 cal/cm$^2$, shield 50 mils aluminum, copper wires, 10Ω loads. $R_s$ (Figure 1) = 1.2 cm.

22

While no examples are given, it is evident that <u>aluminum</u> wires will lead to smaller $|V_{ij}|$ due to an emission yield smaller than that of copper (Table 1). Additionally, the smaller attenuation through aluminum wires (Table 1) will tend to reduce the "voltage source imbalance" between wires of a pair at any angle of incidence, also tending to reduce $|V_{ij}|$.

### 2.2.3    Shield With Vacuum Gap $R_s$-$R_b$

Consider now the case of a vacuum gap between $R_s$ and $R_b$. Capacitance $C_{si}$ in (3) may be reduced considerably, thereby increasing the shield current generator (Figure 2b) $I^*_{si}$. Tables 5b and 8b are appropriate to a shield radius $R_s$ = 1.2 cm ($R_b$ = 1 cm).

The purpose of this example is to illustrate the change in the bundle response due solely to the change in the sheath capacitance. For this reason, the wall emission currents $I_{si}$ are <u>not</u> changed from the previous values appropriate to the "close-in" shield.

At the higher fluence (T5b) the $V_{ij}$ range from ∿1 to 21 volts while the terminal voltages $|V_i|$ reach ∿14 keV. Note that the effect of the wire voltage sources is barely noticeable.

In this case, the large terminal voltages may be expected to cause significant limiting of electron currents traveling from shield to wires. The differential voltages are across 10Ω, so the currents are ≲2 amps leading to  tens of keV were the load resistors changed to 10 kΩ Even with limiting, however, it is likely that several volts may appear across 10Ω loads at the high fluence level.

Tables 8b and 9 compare the response with 10Ω and 10 kΩ loads respectively at the lower fluence (0.1 cal/cm$^2$). The voltages in these cases are not so high as to indicate severe limiting, and again it appears that several volts may be expected across low resistance loads, particularly for a blackbody source temperature ≳5 keV.

23

| Incidence Angle | Voltage Source $V_{ocwi}$ | BB Temp keV | Peak Differential Voltages $V_{ij} = V_i - V_j$ | | | Peak Conductor Voltages | | |
| --- | --- | --- | --- | --- | --- | --- | --- | --- |
| | | | $V_{17}$ | $V_{23}$ | $V_{65}$ | $V_1$ | $V_2$ | $V_5$ |
| 0° | on | 2 | -102 | -129 | -129 | -255 | -228 | -99.6 |
| | | 5 | -839 | -1065 | -1063 | $-2.12^3$ | $-1.90^3$ | - 835 |
| | | 10 | -801 | $-1.03^3$ | $-1.02^3$ | $-2.09^3$ | $-1.86^3$ | - 836 |
| | | 15 | -542 | -703 | -702 | $-1.47^3$ | $-1.30^3$ | - 603 |
| 0° | off | 2 | -103 | -130 | -130 | -256 | -229 | -99.7 |
| | | 5 | -864 | $-1.09^3$ | $-1.09^3$ | $-2.15^3$ | $-1.92^3$ | - 836 |
| | | 10 | -865 | $-1.09^3$ | $-1.09^3$ | $-2.15^3$ | $-1.93^3$ | - 838 |
| | | 15 | -624 | -785 | -784 | $-1.55^3$ | $-1.39^3$ | - 607 |
| 30° | on | 2 | -91.7 | -134 | -54.0 | -283 | -248 | - 226 |
| | | 5 | -769 | $-1.11^3$ | -453 | $-2.36^3$ | $-2.06^3$ | $-1.88^3$ |
| | | 10 | -770 | $-1.07^3$ | -454 | $-2.32^3$ | $-2.03^3$ | $-1.84^3$ |
| | | 15 | -555 | -735 | -327 | $-1.64^3$ | $-1.42^3$ | $-1.29^3$ |
| 60° | on | 2 | -84.6 | -43.6 | -43.4 | -228 | -106 | - 206 |
| | | 5 | -694 | -366 | -364 | $-1.89^3$ | -888 | $-1.71^3$ |
| | | 10 | -655 | -367 | -365 | $-1.85^3$ | -891 | $-1.67^3$ |
| | | 15 | -436 | -264 | -263 | $-1.30^3$ | -644 | $-1.17^3$ |

Table 9. Cable Response. Incident fluence 0.1 cal/cm$^2$, shield 50 mils aluminum, copper wires, 10 kΩ loads. $R_s$ (Figure 1) = 1.2 cm.

24

## 2.2.4     Unshielded Bundle Adjacent to a Plane Wall

Examination of the "voltage source on-off" cases in Tables 5b, 8b, and 9 for the bundle within a gapped shield reveals that to a very adequate approximation in the different voltages, the individual wire sources may be neglected with respect to the shield drivers. This fact allows a similar approximate treatment of the unshielded bundle adjacent to a (flat) electron emitting wall.

The problem geometry is shown in Figure 4. The seven-wire is identical to that previously considered, including the termination configuration of Figure 3.
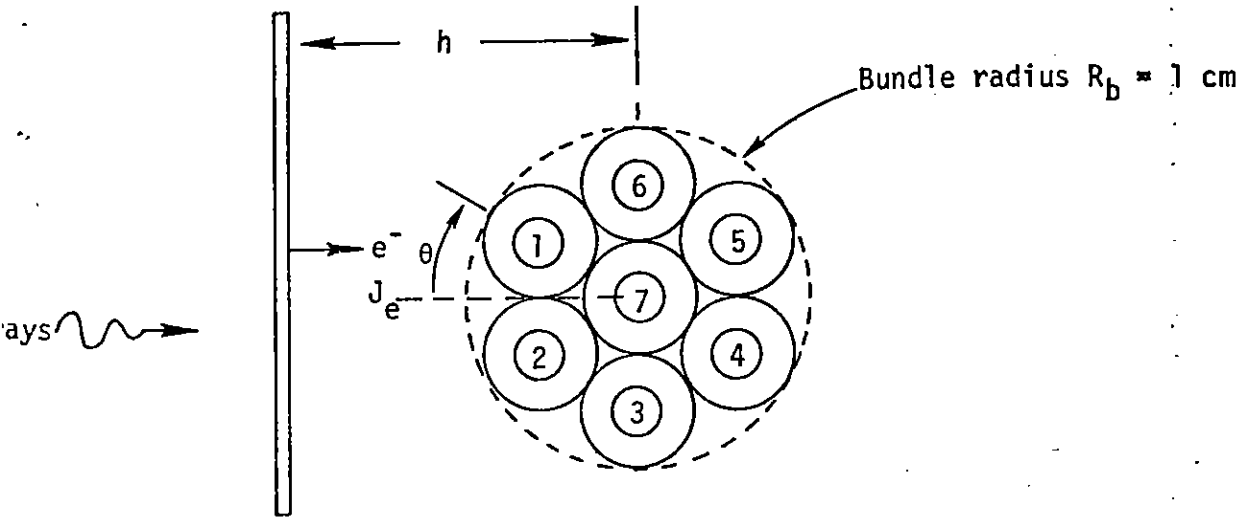
Figure 4. Unshielded seven-wire bundle adjacent to electron emitting wall.

As before, we subdivide the bundle rim into six sections and use equation (2) to find the "new" capacitance to ground. In this case the exterior capacitances are

$$C_{si} = \frac{1}{6} \frac{2\pi\varepsilon_o}{\cosh^{-1}(h/R_b)} \tag{13}$$

In the results to follow, the capacitance of the central wire was treated in the coaxial approximation used previously. We have observed in other calculations regarding the Figure 4 model (same range of emission currents as below) that "turning off" the center wire source makes no

detectable difference in the results. Thus, the latter approximation is not all critical since $\sum\limits_{j=1}^{6} C_{ij}$ is small due to the effective shielding of the outer wires. Also, for these calculations, the large electron layer capacitances in series with (13) are neglected.

The primary effect of interest here is the sensitivity of resultant differential voltages to assumptions regarding the distribution of knock-on electrons over the outer wires.

The IRT PC code has been used to compute the angular distribution of knock-on electrons impacting the surface of a solid wire replacing the bundle of Figure 4, for various standoff distances and wall emission currents. This code incorporates space change limiting and limiting due to a load in the external circuit. In this work we use the PC code data in a simplified manner and make no attempt to include loads to ground in the bundle equivalent to the IRT loading of the (infinite) wire. We further assume in all cases that

$$J_{pk}(\theta) = J_{pk}(0)\cos\theta, |\theta| \lesssim 90°$$
$$= 0 \qquad |\theta| > 90° \tag{14}$$

where $J_{pk}(0)$ is the peak knock-on current density at $\theta = 0$ from the IRT data, for given $J_e$ and $h/R_b$ (Figure 4). The time history of $J_{knock-on}$ is again chosen to be (12).

We consider two distributions of (14) over wires 1, 2, 3 and 6 (Figure 4), in defining the current generators $I_{si}$ as in Figure 2b. Using (14) as is, we assume that

$$I_{s1} = I_{s2} = R_b \int_0^{60°} J_{pk}(\theta) \, d\theta = .866 \ R_b J_{pk}(0)$$

$$I_{s3} = I_{s6} = R_b \int_{60°}^{90°} J_{pk}(\theta) \, d\theta = .134 \ R_b J_{pk}(0) \quad . \tag{15}$$

The uniform distribution is just

$$I_{si} = 1/4 \ [2R_b J_{pk}(0)]. \tag{16}$$
$$i = 1,2,3,6$$

| $J_e \frac{amp}{cm^2}$ | $\frac{J_{pk}(0°)}{J_e}$ | $h/R_b$ | Peak Differential Voltages $V_{ij} = V_i - V_j$ | | | Peak Terminal Voltages $V_i$ | | | | Peak Voltage Drop $\bar{V}_i$ Across R in RLC load | | | | | | |
|---|---|---|---|---|---|---|---|---|---|---|---|---|---|---|---|---|
| | | | $V_{17}$ | $V_{23}$ | $V_{65}$ | $V_1$ | $V_2$ | $V_4$ | $V_5$ | $\bar{V}_1$ | $\bar{V}_2$ | $\bar{V}_3$ | $\bar{V}_4$ | $\bar{V}_5$ | $\bar{V}_6$ | $\bar{V}_7$ |
| 10 | 1.0 | 2 | 8.8 | 21 | 72 | $-2.6^5$ | $-2.8^5$ | $-2.4^5$ | $-2.5^5$ | $5.3^3$ | $5.6^3$ | $5.6^3$ | $4.8^3$ | $5.0^3$ | $5.0^3$ | $5.3^3$ |
| 10 | 1.2 | 5 | 41 | 25 | 89 | $-4.3^5$ | $-4.5^5$ | $-4.0^5$ | $-4.1^5$ | $8.6^3$ | $9.0^3$ | $9.0^3$ | $8.0^3$ | $8.3^3$ | $8.3^3$ | $8.6^3$ |
| 1 | 1.28 | 2 | 1.1 | 2.7 | 9.3 | $-3.4^4$ | $-3.6^4$ | $-3.1^4$ | $-3.2^4$ | 670 | 710 | 710 | 610 | 640 | 640 | 670 |
| 1 | 1.18 | 5 | 4.1 | 2.5 | 8.7 | $-4.2^4$ | $-4.4^4$ | $-3.9^4$ | $-4.0^4$ | 840 | 880 | 880 | 780 | 810 | 810 | 840 |
| .1 | 1. | 2 | .0088 | .021 | .072 | -260 | -280 | -240 | -250 | 5.3 | 5.6 | 5.6 | 4.8 | 5.0 | 5.0 | 5.3 |
| .1 | 1. | 5 | .034 | .021 | .074 | -350 | -370 | -330 | -340 | 7.1 | 7.5 | 7.5 | 6.7 | 6.9 | 6.9 | 7.1 |

Table 11. Response of seven-wire bundle as in Table 10 for uniform charge distribution; all wires have loads to ground (both ends) of (R = 10 kΩ, L = 0.01 h, C = 2 pf).

29

Peak Voltage Drop $\bar{V}_i$ / Peak Terminal Voltages $V_i$ / Peak Differential Voltages $V_{ij}=V_i-V_j$

| $J_e$ $\frac{amp}{cm^2}$ | $\frac{J_{pk}(0°)}{J_e}$ | $\frac{h}{R_b}$ | $V_{17}$ | $V_{23}$ | $V_{65}$ | $V_1$ | $V_2$ | $V_4$ | $V_5$ | $\bar{V}_1$ | $\bar{V}_2$ | $\bar{V}_3$ | $\bar{V}_4$ | $\bar{V}_5$ | $\bar{V}_6$ | $\bar{V}_7$ |
|---|---|---|---|---|---|---|---|---|---|---|---|---|---|---|---|---|
| 10 | 1.0 | 2 | $-5.4^2$ | $-4.4^2$ | $-3.9^2$ | $-1.6^5$ | $-1.7^5$ | $-7.4^4$ | $-1.4^5$ | $4.5^3$ | $4.8^3$ | $4.8^3$ | $1.8^2$ | $4.2^3$ | $4.2^3$ | $4.4^3$ |
| 10 | 1.2 | 5 | $-8.0^2$ | $-7.0^2$ | $-6.5$ | $-1.9^5$ | $-2.1^5$ | $-6.4^4$ | $-1.7^5$ | $6.8^3$ | $7.2^3$ | $7.2^3$ | $2.8^2$ | $6.5^3$ | $6.5^3$ | $6.8^3$ |
| 1 | 1.28 | 2 | $-69$ | $-56$ | $-50$ | $-2.0^4$ | $-2.2^4$ | $-9.4^3$ | $-1.8^4$ | $5.7^2$ | $6.1^2$ | $6.1^2$ | $23$ | $5.4^2$ | $5.4^2$ | $5.7^2$ |
| 1 | 1.18 | 5 | $-79$ | $-69$ | $-64$ | $-1.9^4$ | $-2.1^4$ | $-6.9^3$ | $-1.8^4$ | $6.7^2$ | $7.1^2$ | $7.1^2$ | $27$ | $6.4^2$ | $6.4^2$ | $6.6^2$ |
| .1 | 1. | 2 | $-.54$ | $-.44$ | $-.39$ | $-160$ | $-170$ | $-74$ | $-140$ | $4.5$ | $4.8$ | $4.8$ | $.18$ | $4.2$ | $4.2$ | $4.4$ |
| .1 | 1. | 5 | $-.67$ | $-.59$ | $-.54$ | $-160$ | $-176$ | $-53$ | $-141$ | $5.6$ | $6.0$ | $6.0$ | $.23$ | $5.4$ | $5.4$ | $5.6$ |
| **uniform cosθ** | | | | | | | | | | | | | | | | |
| 10 | 1.0 | 2 | $-4.9^2$ | $-3.6^2$ | $-4.2^2$ | $-1.6^5$ | $-1.8^5$ | $-7.4^4$ | $-1.3^5$ | $4.6^3$ | $4.9^3$ | $4.9^3$ | $1.8^2$ | $3.9^3$ | $3.9^3$ | $4.6^3$ |
| 10 | 1.2 | 5 | $-7.4^2$ | $-6.0^2$ | $-6.8^2$ | $-2.0^5$ | $-2.2^5$ | $-6.4^4$ | $-1.6^5$ | $7.0^3$ | $7.4^3$ | $7.3^3$ | $2.8^3$ | $6.1^3$ | $6.1^3$ | $7.0^3$ |
| 1 | 1.28 | 2 | $-63$ | $-45$ | $-53$ | $-2.1^4$ | $-2.3^4$ | $-9.5^3$ | $-1.7^4$ | $600$ | $628$ | $625$ | $23$ | $500$ | $510$ | $590$ |
| 1 | 1.18 | 5 | $-72$ | $-60$ | $-67$ | $-2.0^4$ | $-2.1^4$ | $-6.3^3$ | $-1.5^4$ | $690$ | $720$ | $720$ | $27$ | $600$ | $600$ | $690$ |
| .01 | 1. | 2 | $-.49$ | $-.35$ | $-.42$ | $-160$ | $-180$ | $-74$ | $-130$ | $4.7$ | $4.9$ | $4.9$ | $.18$ | $3.9$ | $3.9$ | $4.6$ |
| .01 | 1. | 5 | $-.61$ | $-.50$ | $-.57$ | $-170$ | $-180$ | $-53$ | $-131$ | $5.8$ | $6.1$ | $6.1$ | $.23$ | $5.1$ | $5.1$ | $5.8$ |

Table 10. Response of seven-wire bundle adjacent to emitting ($J_e$) plane wall (Figure 4).

$J_{pk}(0°)$ is peak knock-on electron current density from IRT PC code for a solid wire of radius $R_b$ at a standoff distance h. The knock-on charge is distributed either uniformly or by cos θ over wires 1, 2, 3, and 6. The interwire terminal loads are 10 Ω. The loads to ground (both ends) are (R = 0.5 Ω, L = 10 μh, C = 2 pf: wire 4) and (R = 10 kΩ, L = 0.01 h, C = 2 pf) for all other wires.

28

## Section 3

## COMPARISON OF MULTICONDUCTOR CABLE CODES

### Paul Trybus

The transient response of a multiconductor cable is solved with either a distributed parameter model (like MCABLE) or a lumped parameter model of the cable and a circuit code like SCEPTRE.

For straight cables MCABLE computes the solution significantly faster than the lumped parameter model. However, MCABLE does not allow cable bends that can easily be a part of real cable.

In this subtask we examine the increase in computer core and in computer time that would accompany the alteration of the MCABLE code to handle cable bends; the resultant code was called BCABLE.

### 3.0 MCABLE

MCABLE is a uniform multiconductor transmission code that solves the telegraphers equations in the time domain. For this study a seven wire configuration was used (Figure 5). Forty nodes over the 1 meter length resulted in a $\Delta x$ = 2.5 cm. Licking's capacitance code [4] calculated the capacitance matrix which was then used to create the associated inductance matrix. A dielectric constant of 2.5 was associated with the cable. A plane-wave E field drove the cable, incident tangentially. The form of the field was a unit $sin^2$ pulse of 10 ns duration. Core requirements were 43K (octal) and 163 CPU secs for a time duration of 100 ns on a CDC 6600 machine.

Figures 6 and 7 show the termination conditions of the cable and Figures 8 and 9 present bulk currents at each end of the cable.

31

The $\overline{V}_i$ in Tables 10 and 11 are peak values of

$$\overline{V}_i(t) = -\frac{R}{L} e^{-tR/L} \int_o^t e^{tR/L} V(t')dt' \quad , \tag{17}$$

the voltage drop across the load resistor R in the RLC terminations to ground at the wire ends. It is evident from the tables that the currents to ground $\overline{V}_{i/R}$ may be quite substantial at high fluence levels.
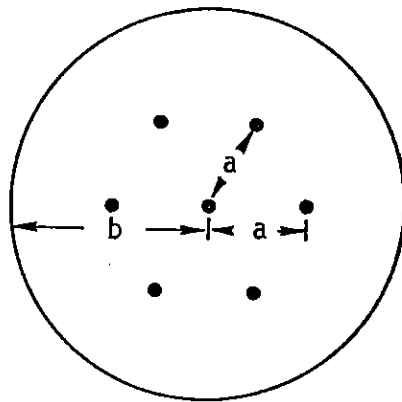
Wire Radii = 2.533 mm
a = 6.666 mm
b = 10. mm

Figure 5.  Seven-Wire Configuration

## 3.1 BCABLE

BCABLE is a modification of MCABLE. A nonuniform or bent 7-wire cable configuration is allowed through the use of distinct capacitance and inductance matrices at each node. For this study the first 38 nodes were taken to be identical to the MCABLE run. The last two nodes used the configuration of Figure 10 to simulate a bent cable. Termination and drives were the same as in the MCABLE run. BCABLE needed 55K (octal) core and 171 CPU secs for the 100 ns time duration. The extra core comes about from the fact that two 7x7 matrices (L and C) are required at each of the 40 nodes. The increased time is due to the additional manipulation that must be done to these distinct L and C matrices, although the increase in time is only 5% over the uniform case.

Figures 11 and 12 present bulk currents for the ends of the bent cable.

A three-wire version of MCABLE was set up and run using a drive on the left end of $e(t) = 10.4 \times 10^4 (e^{-\alpha t} - e^{-\beta t})$ as the source. Figure 13 presents the terminations used at each end. A 40 foot cable. of the geometry presented in Figure 14 took 70 CPU sec and required 36K (octal) for a 900 ns time duration. Figures 15 to 20 present currents for each cable at each end.

32
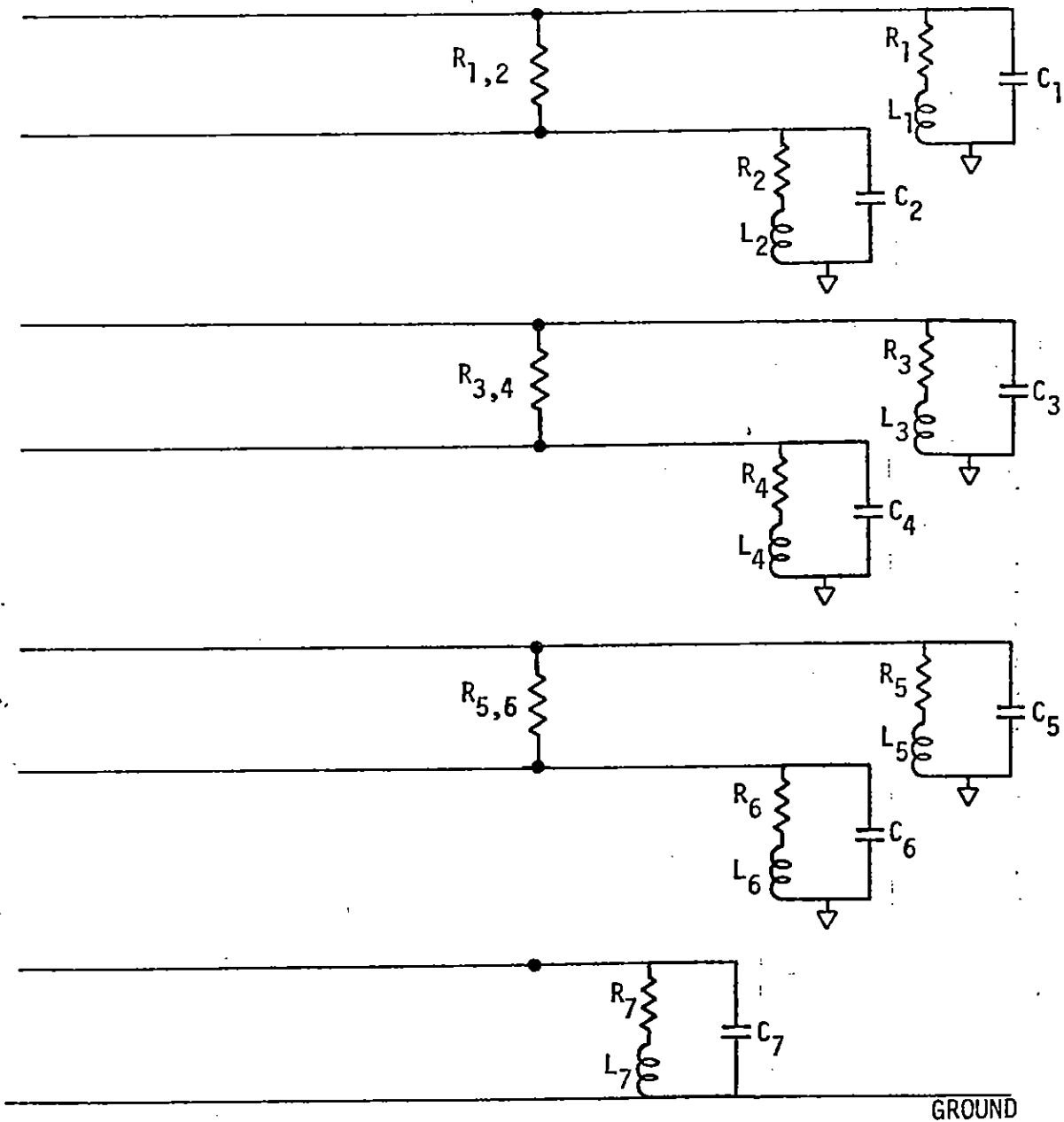
$R_{1,2} = 75\Omega$     $R_{3,4} = 1000\Omega$     $R_{5,6} = 10\Omega$

$C_1 = 6_{pf}$     $C_2 = 20_{pf}$   $C_3 = 15_{pf}$     $C_4 = 7_{pf}$     $C_5 = 30_{pf}$     $C_6 = 3_{pf}$     $C_7 = 1\times10^{-4}_{pf}$

$R_1 = R_2 = R_3 = R_4 = R_5 = R_6 = 1\times10^8\Omega$   $R_7 = 1\times10^{-4}\Omega$

$L_1 = L_2 = L_3 = L_4 = L_5 = L_6 = 100\ H$   $L_7 = 1\times10^{-5}\ H$

Figure 7.   Seven Wires:   Right-End Terminations
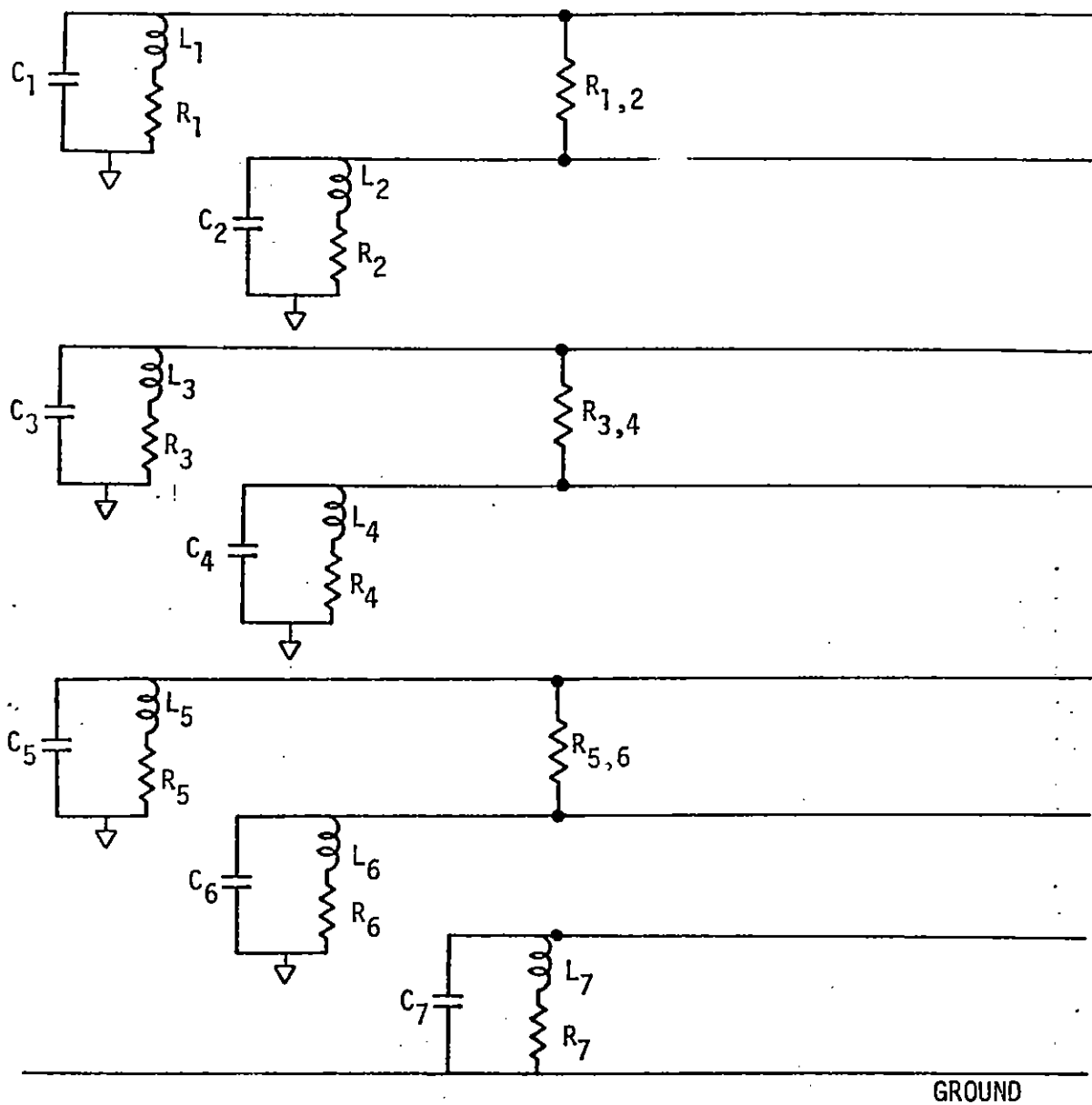
$R_{1,2} = 150\Omega$   $R_{3,4} = 5000\Omega$   $R_{5,6} = 47\Omega$

$C_1 = 10_{pf}$   $C_2 = 5_{pf}$   $C_3 = 12_{pf}$   $C_4 = 7_{pf}$   $C_5 = 20_{pf}$   $C_6 = 6_{pf}$   $C_7 = 1\times10^{-4}_{pf}$

$R_1 = R_2 = R_3 = R_4 = R_5 = R_6 = 1\times10^8\Omega$   $R_7 = 1\times10^{-4}\Omega$

$L_1 = L_2 = L_3 = L_4 = L_5 = L_6 = 100\ H$   $L_7 = 1\times10^{-5}\mu H$

Figure 6.   Seven Wires:   Left-End Terminations

34
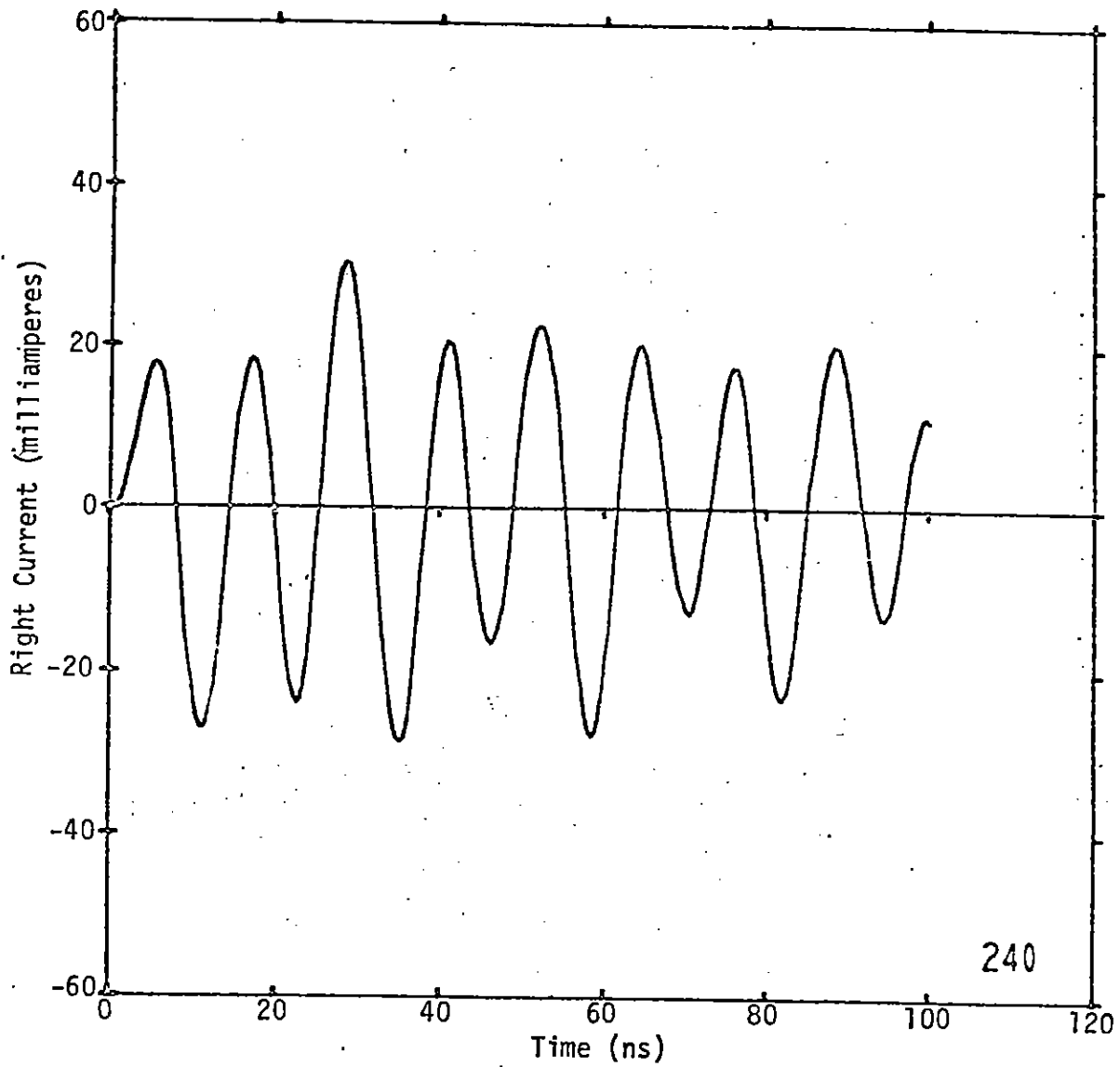
Figure 9. Uniform cable, bulk current, right end.
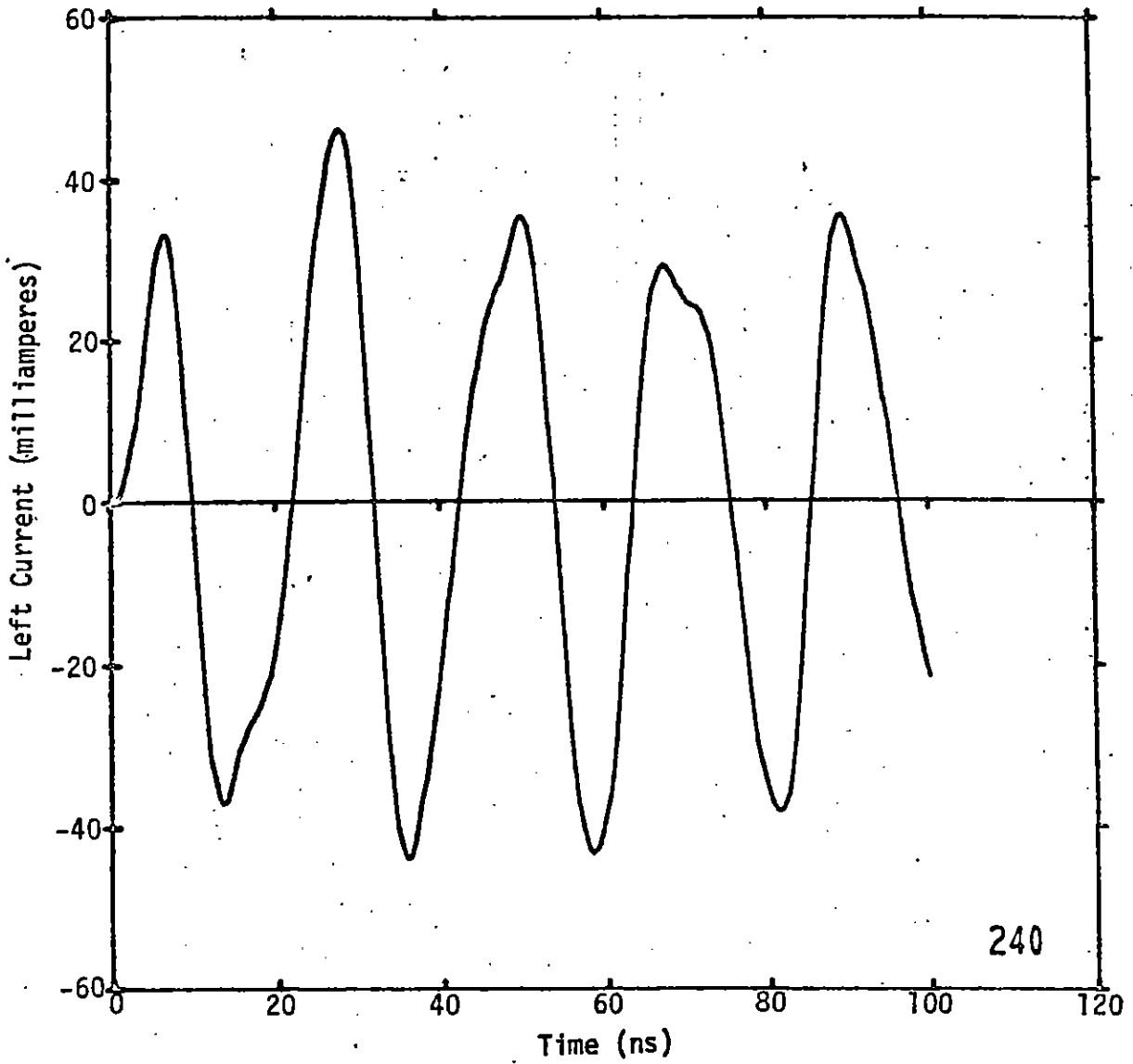
Figure 8.  Uniform cable, bulk current, left end.
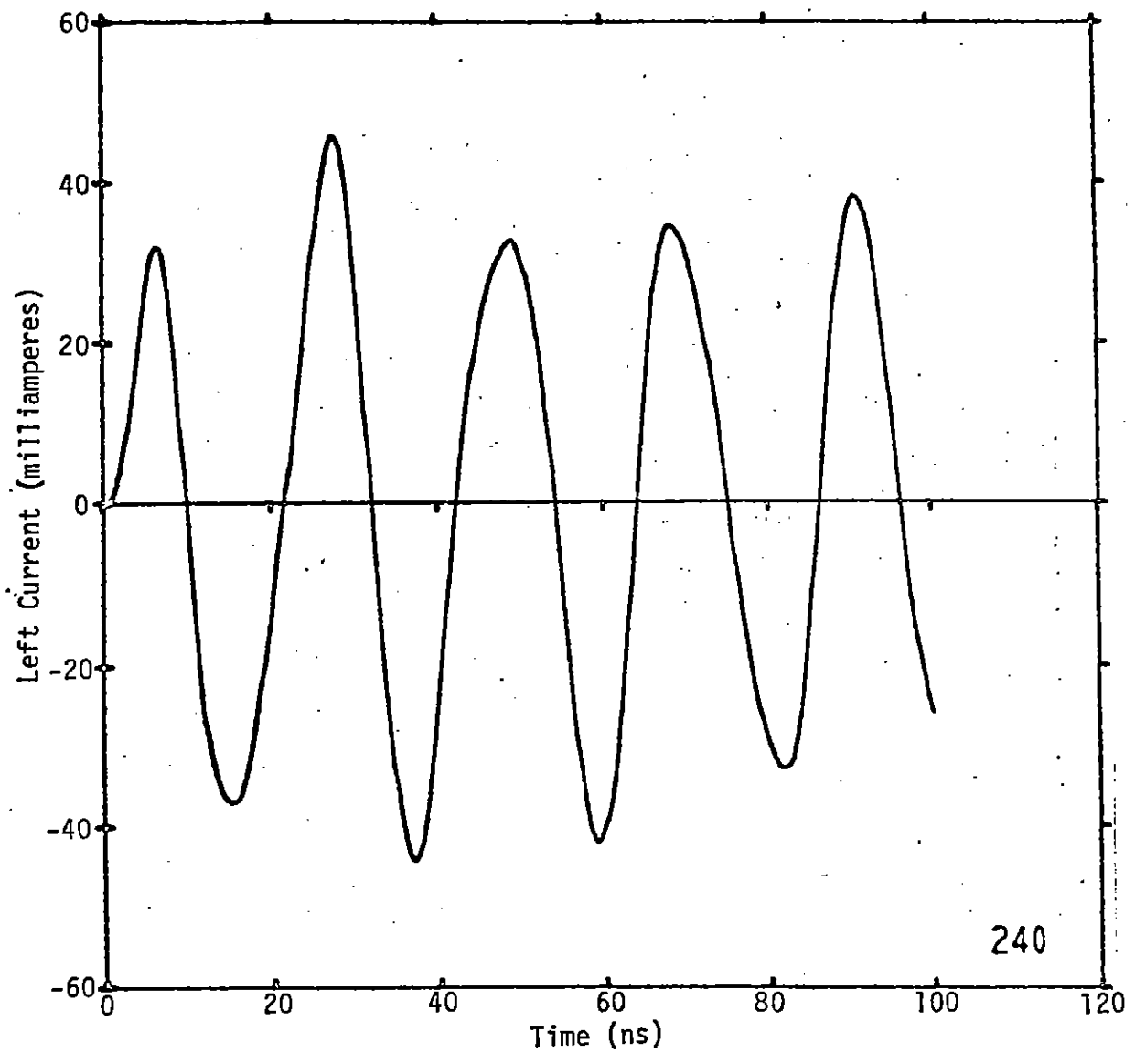
Figure 11. Bent cable, bulk current, left end.

Wire radii = 2.533 mm
a = 6.666 mm
b = 100. mm

Cable Simulated
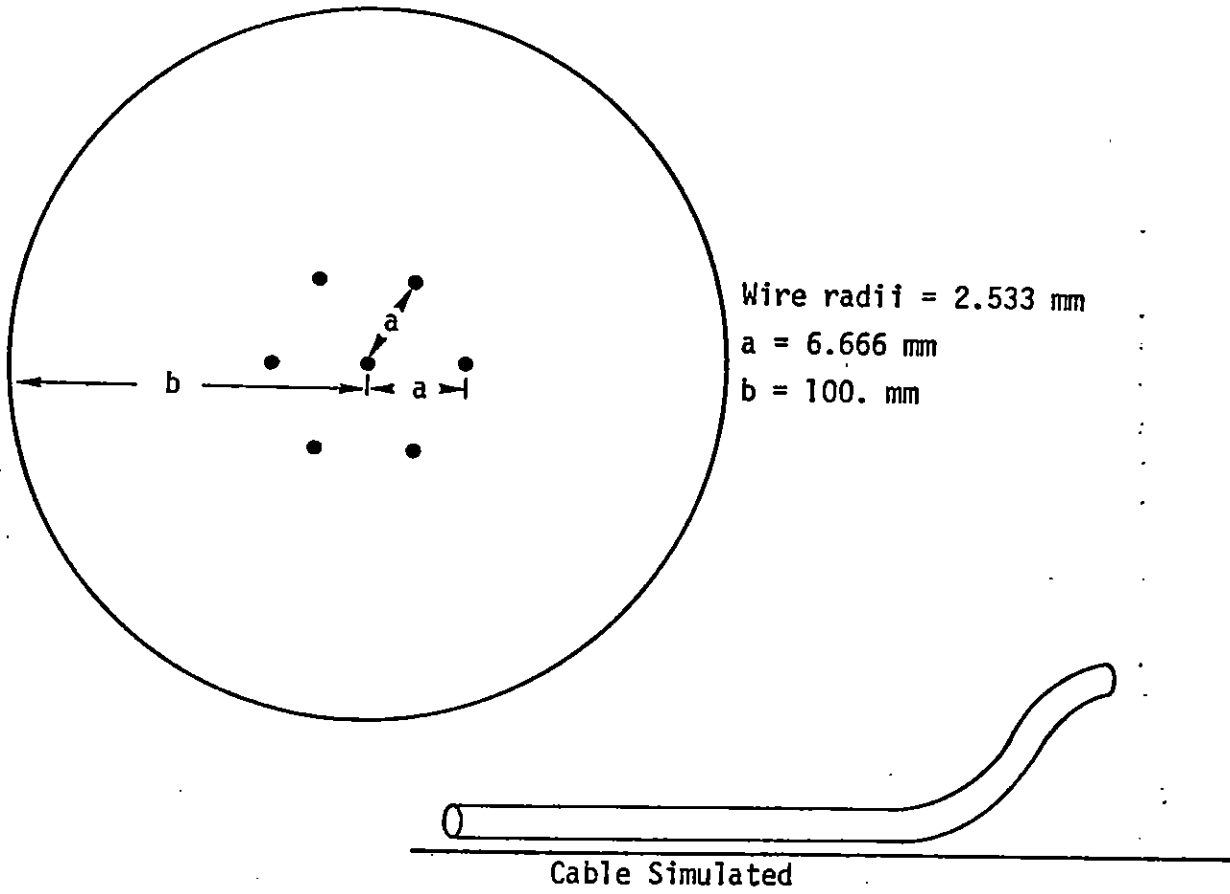
Figure 10. Bent Seven-Wire Configuration

$R_1 = R_2 = R_3 = 0.1\Omega$

$L_1 = L_2 = L_3 = 3\times10^{-7}$ H

$C_1 = C_2 = C_3 = 7.36\times10^{-12}$ F

$R_{1,2} = 3.3\Omega$
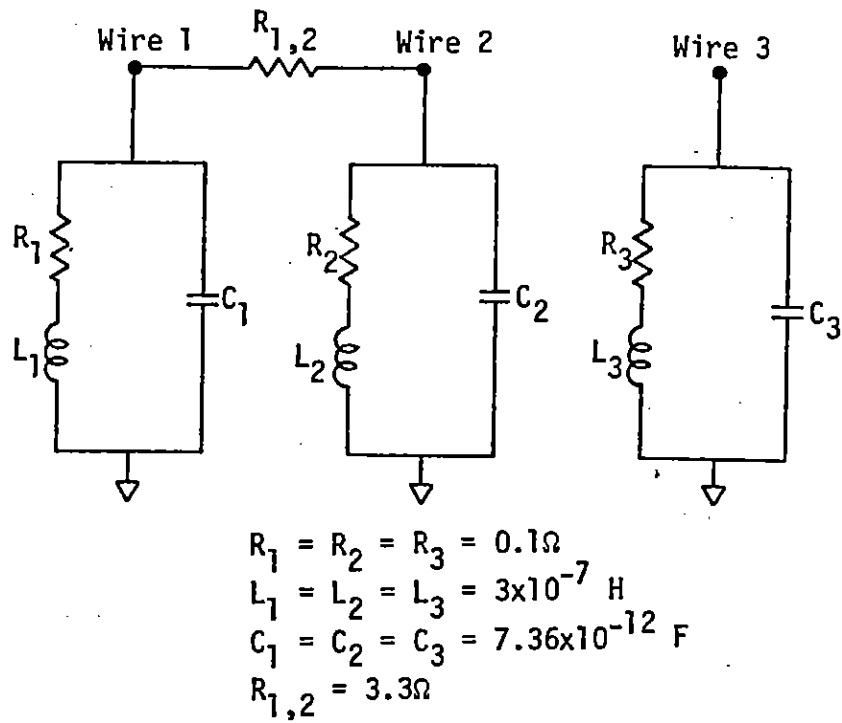
Figure 13.   Three-wire terminations (left and right ends).
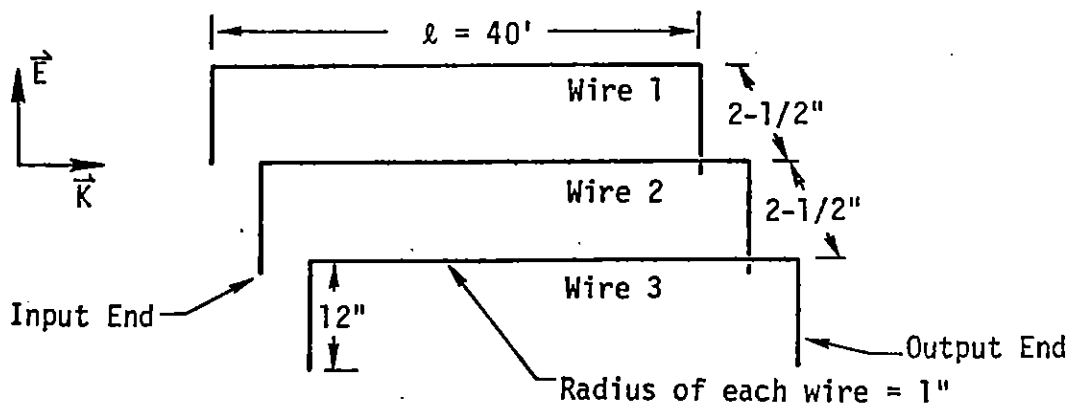


Figure 14.   Cable Geometry (not to scale)
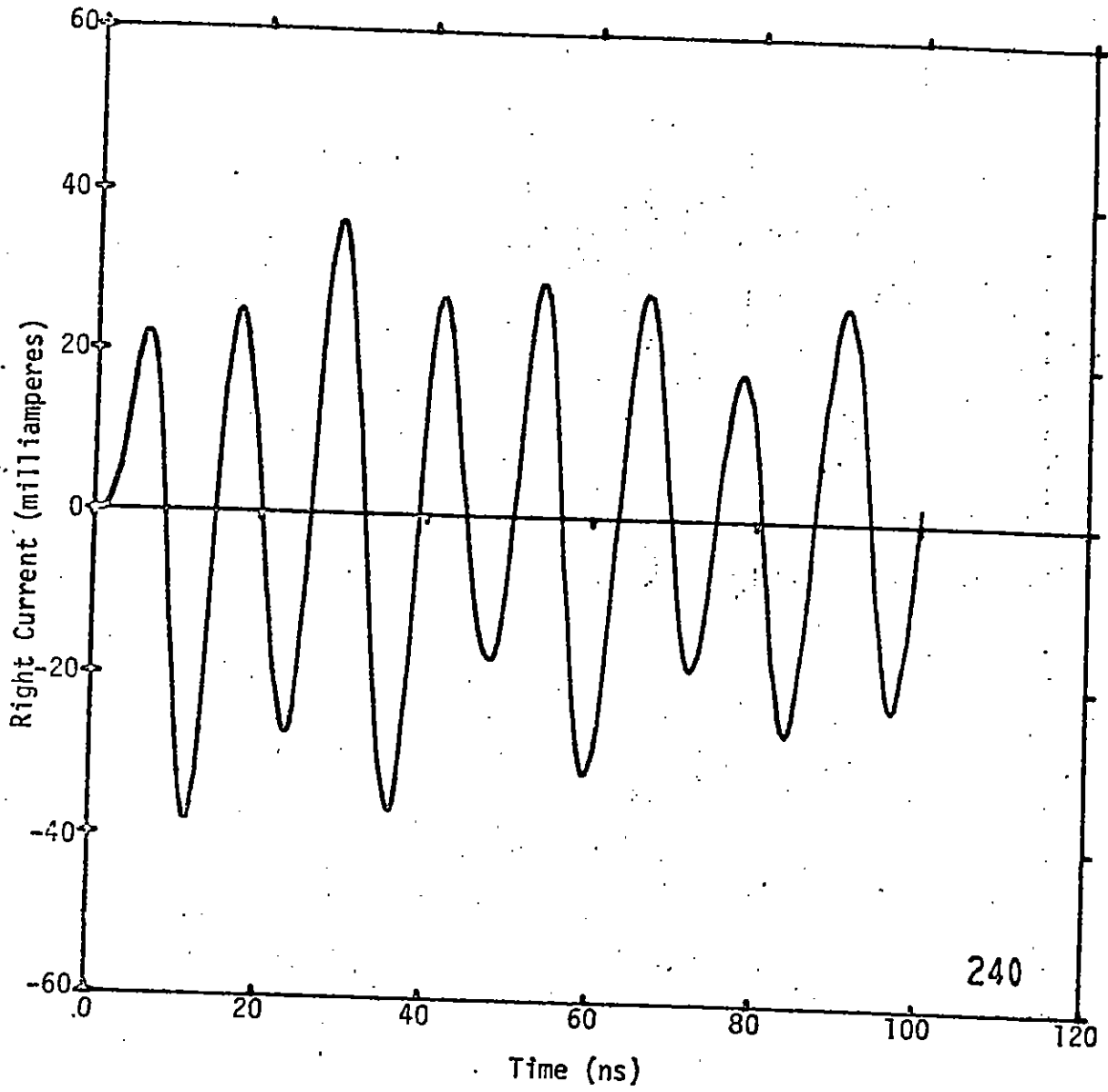
Figure 12. Bent cable, bulk current, right end.
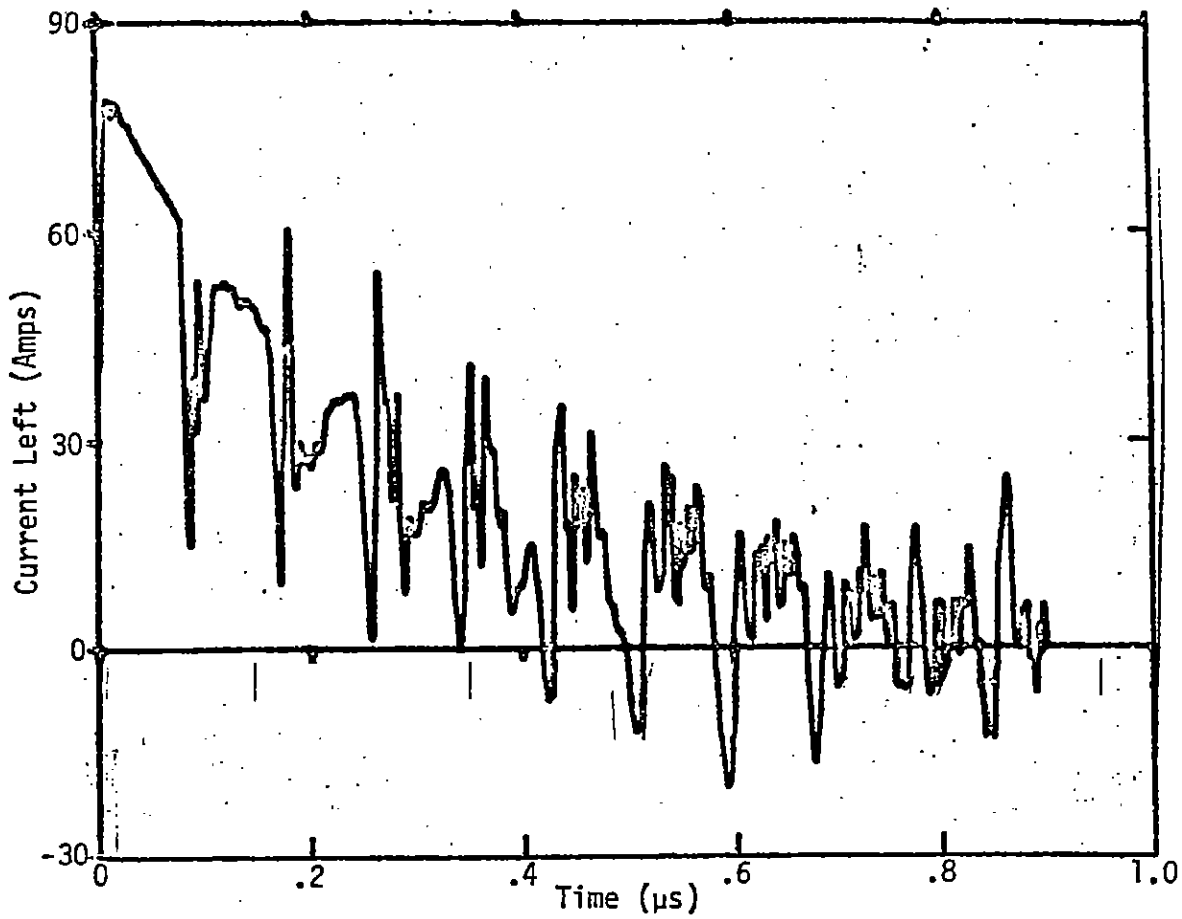
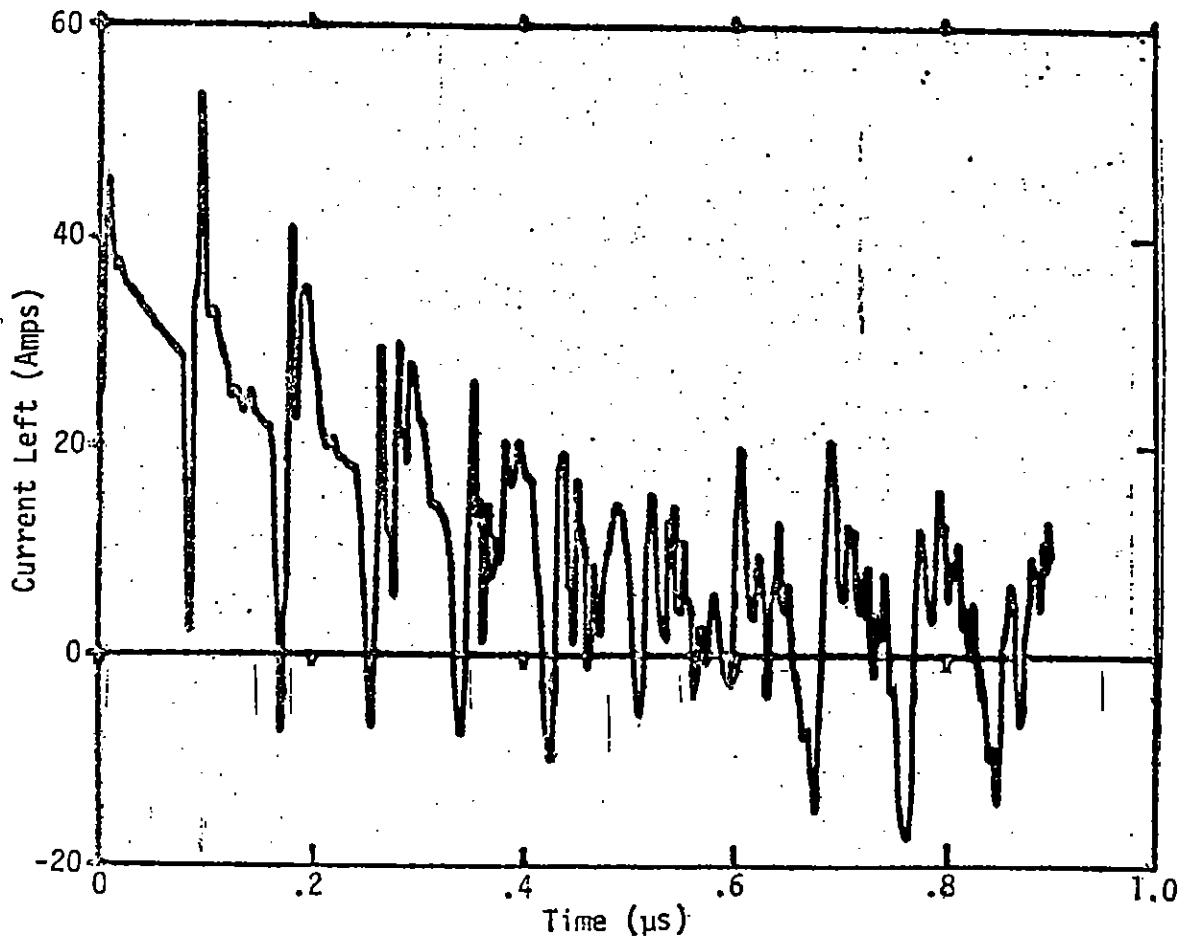Figure 17. Wire 3



Figure 18. Wire 1

43
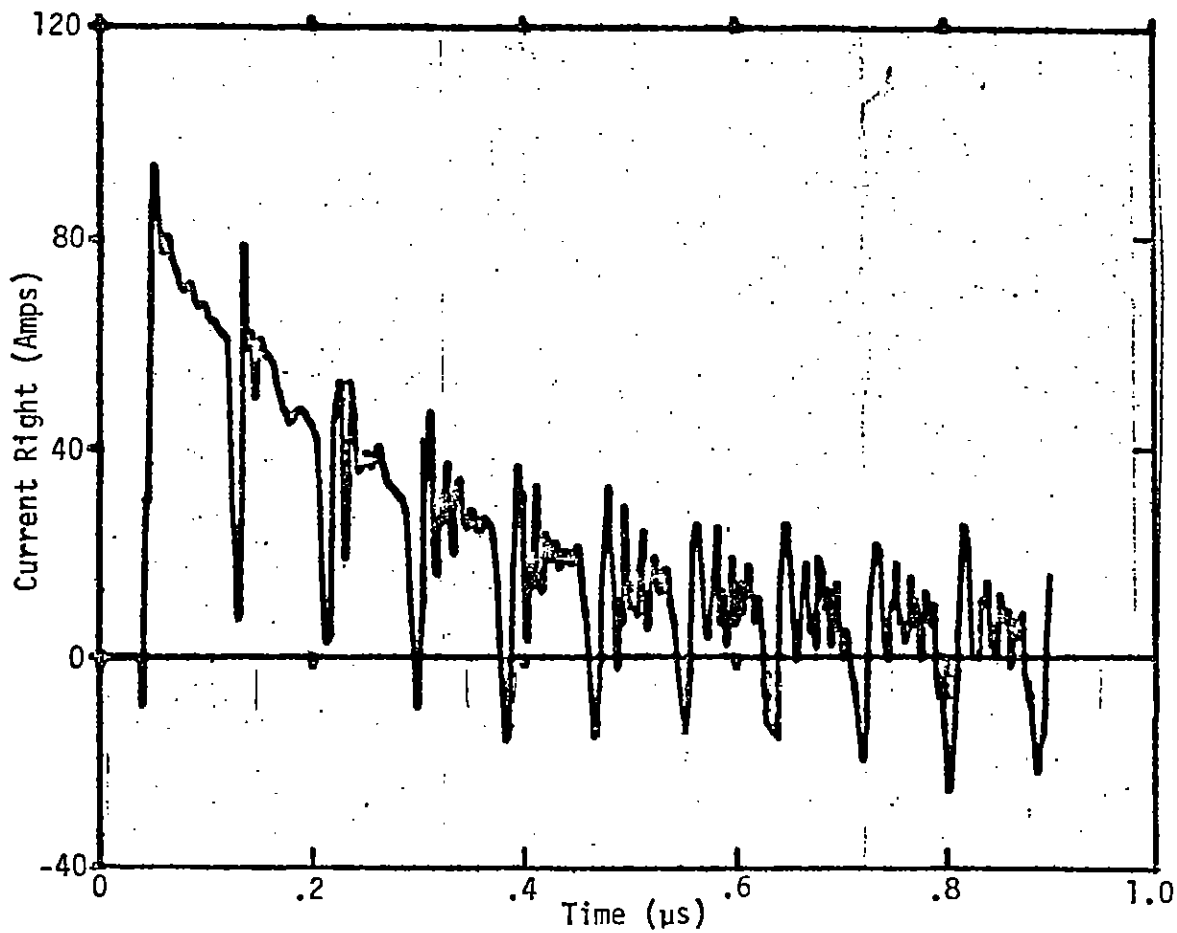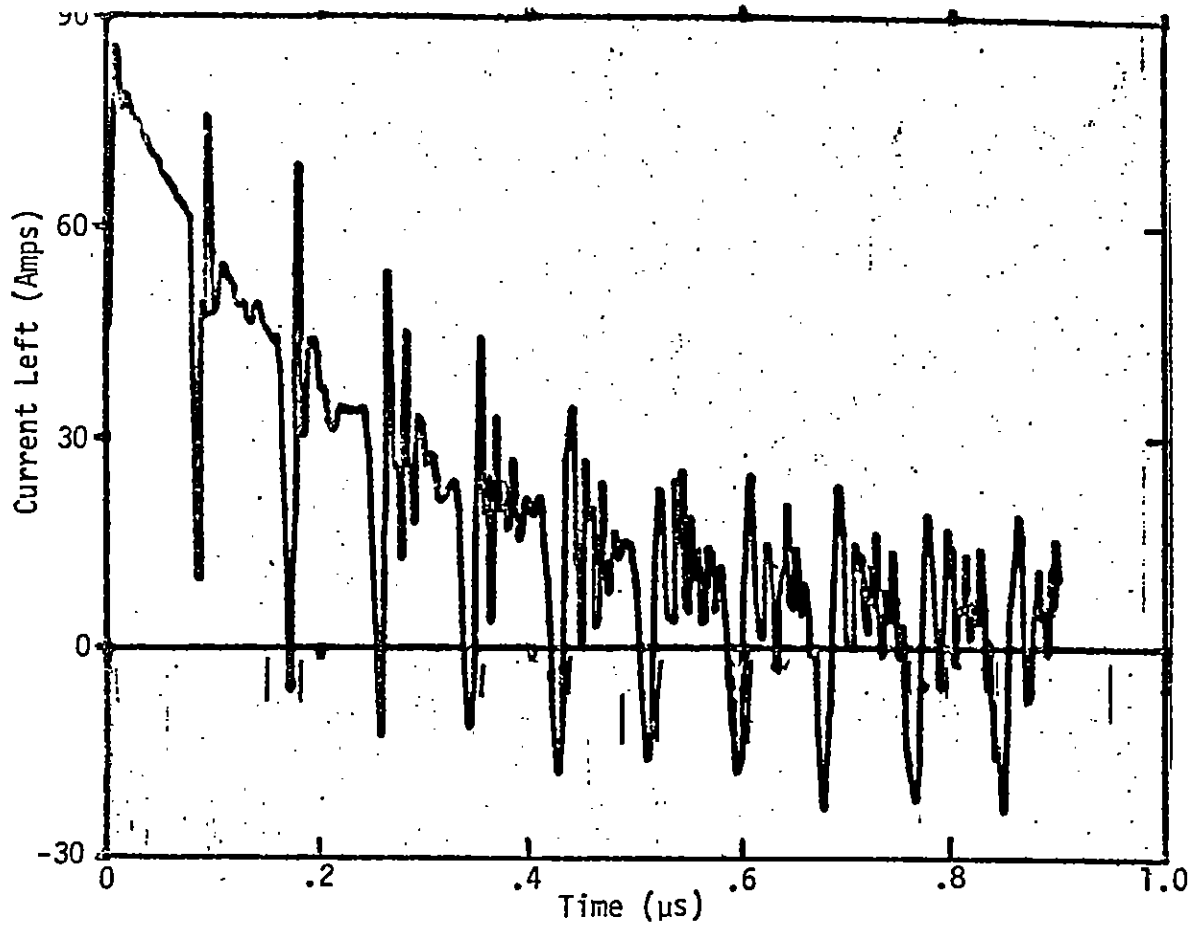
Figure 15.  Wire 1



Figure 16.  Wire 2

42

# Section 4

## MAGNETIC TURNING EFFECTS AND CABLE RESPONSE

### Monti Wilson

Consider a wire of radius ~few tenths cm located several cm from a ground plane. If the turning of electrons in the H field due to the wire current is to have a significant self-consistent effect on the wire current, then the electron Larmor radius must be comparable to the wire standoff distance. The Larmor radius is

$$R(cm) = 8.48 \times 10^3 \frac{V}{H}^{\frac{1}{2}} \, ,$$

where $\overline{V}$ = electron kinetic energy (kev) and H = magnetic field intensity (Amp/m).

Assuming the maximum H at the surface of a wire of radius r(cm) for estimation purposes, the Larmor radius given a wire current I (Amps) is

$$R(cm) = \frac{533 r \overline{V}^{\frac{1}{2}}}{I} \, .$$

Some typical values of R are shown in Table S1, assuming a wire radius r = 0.2 cm.

| I(Amp) | $\overline{V}$(kev) | | | |
|---|---|---|---|---|
| | 1 | 10 | 30 | 100 |
| 10 | 10.6 | 33.7 | 58.4 | 105 |
| 50 | 2.12 | 6.74 | 11.7 | 21 |
| 100 | 1.06 | 3.37 | 5.84 | 10.7 |
| 500 | .212 | .67 | 1.17 | 2.13 |

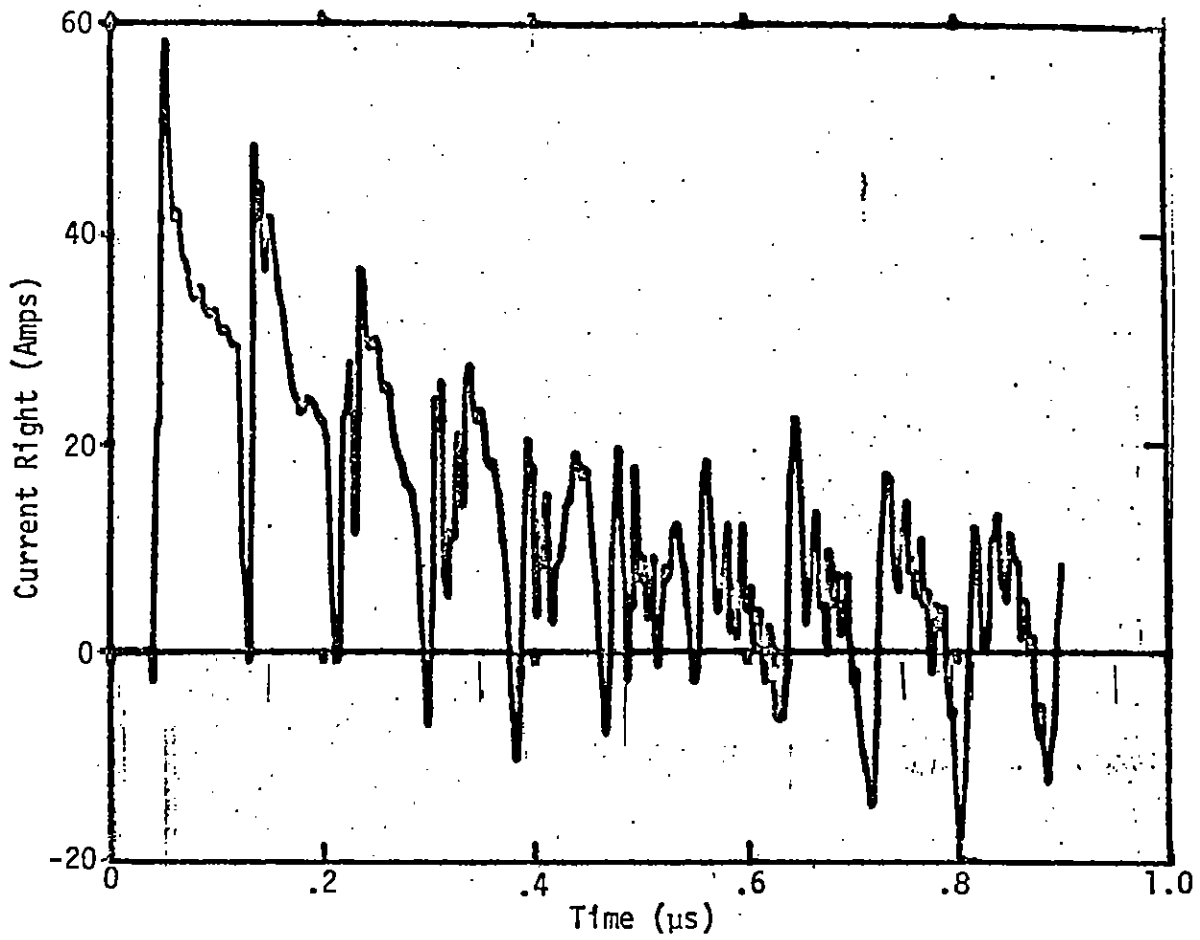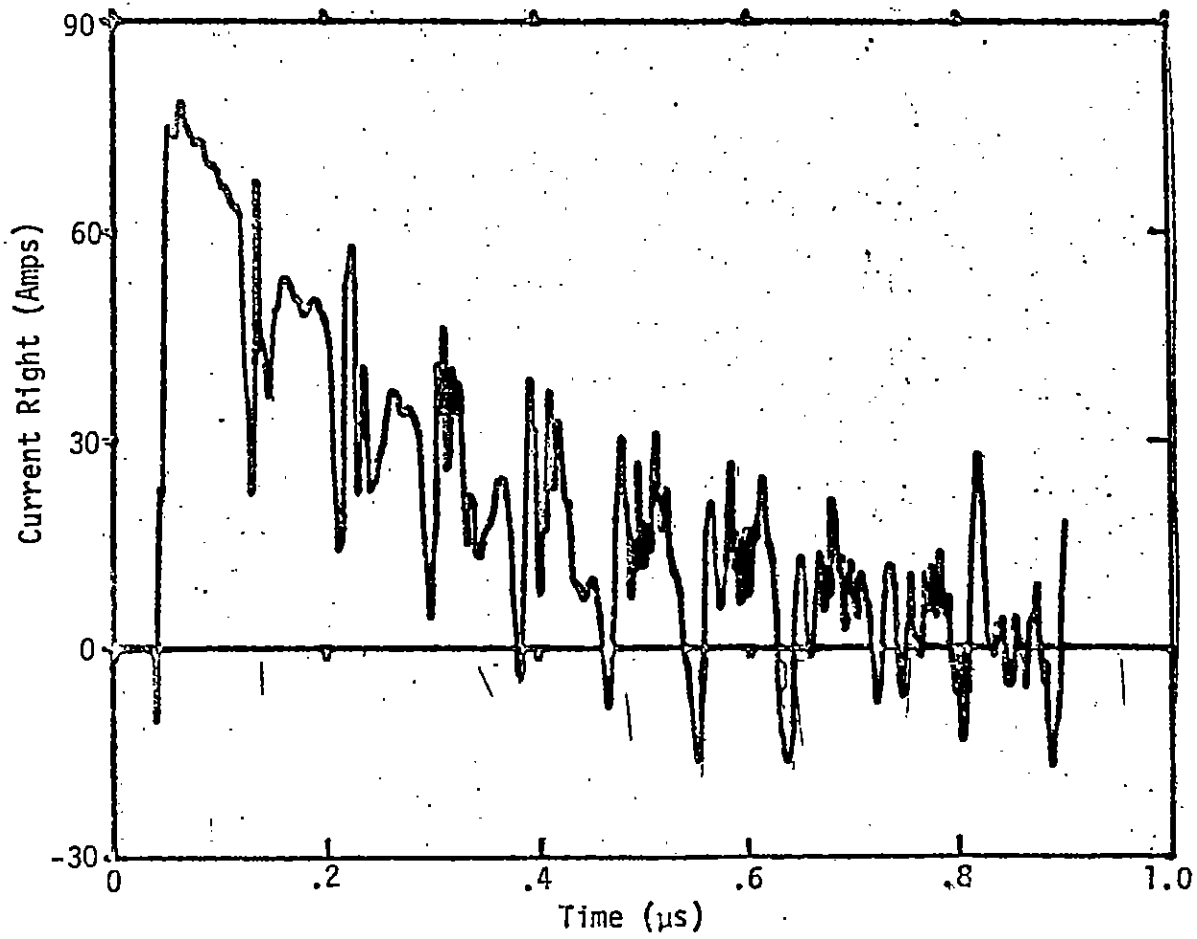Table 12. Entries are R(cm).

Figure 19.  Wire 2



Figure 20. Wire 3

44

# REFERENCES

1.  Dellin, T. A. and C. J. MacCallum, "A Handbook of Photo-Compton Current Data," Sandia Laboratories, SCL-RR-720086, December 1972.

2.  Dellin, T. A. and C. J. MacCallum, "QUICKE2: A One-Dimensional Code for Calculating Bulk and Vacuum Emitted Photo-Compton Currents," Sandia Laboratories, SLL-74-0218, April 1974.

3.  Trybus, P. and D. E. Merewether, "Time Domain Solution of Multiconductor Transmission Line Coupling Problems," AMRC-R-21, Mission Research Corp., January 1974.

4.  Licking, L. D., "Capacitance Analysis for Arbitrary Cylindrical Geometries: Application to Electromagnetic Coupling into Subsystems Through Cables," Sandia Laboratories, SC-RR-72-0299, June 1972.

5.  Ezell, T. F., "Capacitance Coefficients for Shielded Multiwire Cables," Preliminary Draft, November 1973.

6.  Berger, M. J. et al., "Tables of Energy Losses and Ranges of Electrons and Positrons," National Aeronautics and Space Administration, N65-12506, Washington, D. C., 1964.

Thus, for cable currents $\lesssim 50$ Amp and electron kinetic energies $\sim 10$-$30$ keV, it appears that magnetic turning cannot have an important effect on cable response. Better estimates of J turning effects could be made through modification of existing quasistatic 2-d particle codes for predicting radiation induced cable response; however, there seems to be little reason to do so.